



日本原子力研究開発機構機関リポジトリ  
Japan Atomic Energy Agency Institutional Repository

Title	Creep-fatigue evaluation method for weld joint of Mod.9Cr-1Mo steel, 2; Plate bending test and proposal of a simplified evaluation method
Author(s)	Ando Masanori, Takaya Shigeru
Citation	Nuclear Engineering and Design,310,p.217-230
Text Version	Author's Post-print
URL	<a href="https://jopss.jaea.go.jp/search/servlet/search?5057386">https://jopss.jaea.go.jp/search/servlet/search?5057386</a>
DOI	<a href="https://doi.org/10.1016/j.nucengdes.2016.10.025">https://doi.org/10.1016/j.nucengdes.2016.10.025</a>
Right	©2016. This manuscript version is made available under the CC-BY-NC-ND 4.0 license <a href="http://creativecommons.org/licenses/by-nc-nd/4.0/">http://creativecommons.org/licenses/by-nc-nd/4.0/</a>

**Title**

Creep-fatigue evaluation method for weld joints of Mod.9Cr-1Mo steel  
Part II: Plate bending test and proposal of a simplified evaluation method

**Authors**

Masanori Ando

*Japan Atomic Energy Agency, Oarai-cho, Higashi-ibaraki, Ibaraki, 311-1393, Japan*

*ando.masanori@jaea.go.jp*

*TEL; 8129-267-4141, FAX;8129-266-3675*

Shigeru Takaya

*Japan Atomic Energy Agency, Oarai-cho, Higashi-ibaraki, Ibaraki, 311-1393, Japan*

*takaya.shigeru @jaea.go.jp*

## Abstract

In the present study, to develop an evaluation procedure and design rules for Mod.9Cr-1Mo steel weld joints, a method for evaluating the creep-fatigue life of Mod.9Cr-1Mo steel weld joints was proposed based on finite element analysis (FEA) and a series of cyclic plate bending tests of longitudinal and horizontal seamed plates. The strain concentration and redistribution behaviors were evaluated and the failure cycles were estimated using FEA by considering the test conditions and metallurgical discontinuities in the weld joints. Inelastic FEA models consisting of the base metal, heat-affected zone and weld metal were employed to estimate the elastic follow-up behavior caused by the metallurgical discontinuities. The elastic follow-up factors determined by comparing the elastic and inelastic FEA results were determined to be less than 1.5. Based on the estimated elastic follow-up factors obtained via inelastic FEA, a simplified technique using elastic FEA was proposed for evaluating the creep-fatigue life in Mod.9Cr-1Mo steel weld joints. The creep-fatigue life obtained using the plate bending test was compared to those estimated from the results of inelastic FEA and by a simplified evaluation method.

## Keywords

Heat-resistant steel, Weld joint, Fatigue, Creep-fatigue interaction, Elevated temperature

## 1. Introduction

Mod.9Cr-1Mo steel is a candidate material for the primary and secondary heat transport system components in the Japan sodium-cooled fast reactor (JSFR) [1]. A shorter piping layout and rational component design have been planned for the JSFR. To enhance safety and economic competitiveness, the Japan Atomic Energy Agency has proposed an attractive plant concept and extended considerable effort to demonstrate the applicability of innovative technologies to the JSFR. One of the most practical methods for enhancing economic competitiveness is to reduce the construction costs by diminishing the total quantity of required structural materials. To satisfy these requirements, high-Cr ferritic steel has attractive characteristics as the main structural material of sodium-cooled fast reactors (SFRs) because it has both excellent thermal properties and high-temperature strength.

To accommodate the application of this new material, the Japan Society of Mechanical Engineers (JSME) updated the design and construction codes for fast reactors (FRs) in 2012 [2]. The main topic in the 2012 edition of the JSME FRs code was the registration of two new materials: 316FR and Mod.9Cr-1Mo steels. In addition to standardizing the allowable strength values and material properties for registration, the creep-fatigue evaluation procedures and other rules for these new materials were defined. Moreover, the margins for the new materials with respect to the rules were assessed to confirm that the magnitudes of the margins are appropriate for the new materials [3].

The JSME FRs code is based on design guidelines applied to the construction of the Japanese Prototype Fast Reactor “Monju” [4-5] with appropriate updates. The original guidelines did not include a method for evaluating creep-fatigue damage in weld joints because all weld joints for Monju were manufactured far from the areas where the primary and secondary stresses were expected to be significant. Consequently, the JSME FRs code also does not include a method for evaluating creep-fatigue damage in the weld joints. However, the shorter piping layout and optimized component design of the JSFR allows the generation of significant secondary stress under certain events (e.g., plant trips) at the locations of the weld joints. In addition, the individual failure mechanism for Type IV cracking in high-Cr ferritic steel should be considered during piping and component design. Therefore, the development of an evaluation procedure and design rules for Mod.9Cr-1Mo steel weld joints is an important subject for JSFR design.

To evaluate creep rupture strength considering Type IV cracking, creep rupture curves for Mod.9Cr-1Mo steel weld joints [6] have been proposed based on available creep rupture data and the stress range partitioning method [7-8]. Considering these proposed creep rupture curves for Mod.9Cr-1Mo steel weld joints, a provisional welded joint strength reduction factor (WJSRF) for Mod.9Cr-1Mo steel was also proposed. The WJSRF was proposed to be used to develop the rules that limit primary stress in the JSME FRs code.

On the other hand, creep-fatigue is the most important failure mode to be prevented in SFR design. Therefore, we have developed a method for evaluating creep-fatigue in Mod.9Cr-1Mo steel weld joints. In Part I [9], finite element analysis (FEA) considering the three types of materials properties in weld joints such as the base metal (BM), weld metal (WM), and heat-affected zone (HAZ) was performed to evaluate the creep-fatigue life in the uniaxial test. For FEA, these material properties were defined using the obtained test data and data from the open literature [3][10-11]. Using the assumed material properties for FEA with the strain feedback technique enable to simulate the redistribution of stress and strain in a uniaxial creep-fatigue test. On the basis of the calculated FEA results, an original method for evaluating the creep-fatigue life of Mod.9Cr-1Mo steel weld joints was then proposed. With the proposed method, the experimentally determined number of cycles to failure was predicted to be within a factor of 3. In addition to the development of this evaluation method, the strain redistribution behavior was investigated and compared with that estimated using the elastic follow-up method employed in the JSME FRs code. As the results, the elastic follow-up method developed for estimating the strain concentration at structural discontinuities was found to be applicable to the metallurgical discontinuities of Mod.9Cr-1Mo steel weld joints.

In the present study, to validate the evaluation procedure proposed in Part I [9], plate bending tests with weld joints are performed. FEA is then performed considering the test conditions and using the model based on the three materials in weld joints. The material properties for the BM, HAZ, and WM used in the FEA are the same as those used in Part I [9]. In addition, based on the estimated results for the elastic follow-up factor obtained by inelastic FEA, a simplified technique for determining the creep-fatigue life of Mod.9Cr-1Mo steel weld joints based on elastic FEA is proposed.

## 2 Experimental procedures

### 2.1 Materials

The Mod.9Cr-1Mo steel used in this study was normalized at 1050 °C for 30 min and tempered at 780 °C for 30 min. A 32-mm-thick plate was cut and jointed via gas tungsten arc welding to fabricate the weld plate for the tests. After welding, stress relief annealing at 780 °C for 8.4 h was performed before machining the test specimens. The chemical compositions of the BM and WM are summarized in Table 1.

To confirm the properties of the weld joint used in the tests, the Vickers hardness test was performed along the middle line of the thickness using a test force of 49.03 N. The obtained results are shown in Fig.1. The minimum hardness value was  $HV = 196$  for the HAZ, which had an estimated width of approximately 2.5 mm as determined by optical microscopy.

## 2.2 Test specimen and procedures

To clarify the effect of the weld line direction on the crack situation (i.e., location and initiation cycles) and the stress-strain redistribution under the bending load, horizontal and longitudinal welded plates were applied in the tests. Figure 2 shows the specimen used for the plate bending tests. The specimen had a planar portion (length = 30 mm; width = 50 mm; thickness = 10 mm) at its center, and each specimen had eight holes for bolting the plates to the jigs. The plate bending test was performed using a servo-pulsar machine and the jigs. A schematic of the plate bending test is shown in Fig.3. The push-pull force applied using an actuator was converted to the bending force by the jigs and pins. The center of the planar portion was heated to 550 °C using an induction coil heating machine. As a result, the temperature at the edge of the planar portion, which was 15 mm from the longitudinal center of the specimen, was maintained at approximately 530 °C. To consider the temperature distribution in the FEA, temperature was monitored during the test using thermocouples.

The deformation amplitude,  $\delta$ , was defined using the results of a pre-test. In the pre-test, the relationship between  $\delta$  and the strain amplitude at the specimen center was obtained using a strain gauge. Strain ranges of 0.5% and 0.7% were found to correspond to  $\delta$  values of  $\pm 3.145$  mm and  $\pm 4.220$  mm, respectively. Therefore,  $\delta$  values of  $\pm 3.145$  mm and  $\pm 4.220$  mm were used in the tests (Fig.3), and the deformation rate was controlled for the strain rate corresponding to 0.1%/sec. In the creep-fatigue test, deformation was held on one side. Therefore, one side was held at the tension loading and the other side was held at the compression loading.

The tests were interrupted several times to observe crack initiation and propagation in the planar portion using a replica method. For the plate bending test, the numbers of cycles at which a crack appeared on the surface with a length of 1.0 mm,  $N_{1.0\text{ mm}}$ , and at which the load level declined to 25% of the stable cyclic loading level,  $N_{25\% \text{ drop}}$ , were defined as the failure criteria. A crack length of 1.0 mm was selected to ensure visibility in the structural tests. A criterion of 25% load drop was selected because it is used in JIS Z 2279, although it describes the method for the uniaxial fatigue testing. The creep-fatigue life criterion for structural testing has previously been defined as  $N_{1.0\text{ mm}}$  and used to estimate the number of cycles to failure [12-14]. These results have been summarized for the registration of Mod.9Cr-1Mo steel in the JSME FRs code [3], and the results of the present study are compared with these previous results.

Note that because determining whether crack initiation occurred in the HAZ or BM using the replica method was difficult, the location was not explicitly indicated.

## 2.3 Test results

The test conditions and results are summarized in Table 2. The fatigue and creep-fatigue tests were performed with two levels of deformation amplitude ( $\delta = \pm 3.145$  mm and  $\pm 4.220$  mm). In the fatigue tests,  $N_{25\% \text{ drop}}$  and the lower value of  $N_{1.0 \text{ mm}}$  in the BM (HAZ) or WM were obtained because the frequent interruptions required to collect the replicate data prolonged the total test time.

In the fatigue test, the surface crack reached 1.0 mm in the BM before it did in the WM, except in the longitudinal welded plate of the deformation amplitude,  $\delta$ , was  $\pm 4.220$  mm. Several cracks were initiated and propagated during cyclic loading that ultimately joined and resulted in a long crack on the surface.

The relationship between crack propagation and cyclic loading during the creep-fatigue test with  $\delta = \pm 3.145$  mm and holding time of 1.0 h at one side is shown in Fig.4. In both the horizontal and longitudinal welded plates, cracks were detected on the compression holding side at less cycles than these on the tension holding side. Compression holding is known to significantly decrease the number of failure cycles in the creep-fatigue tests of Mod.9Cr-1Mo steel because of oxidation [13][15-28]. This degradation of the creep-fatigue life is caused by the cracking of the oxidation layer. Cracking in the BM is promoted by the cracking of the oxide-layer; however, creep damage is insignificant in the compression side. On the other hand, when the holding time in the test is prolonged, cracks are initiated at less cycles at the tension side than that in the compression side [13][16]. Therefore, the failure criterion to be considered was  $N_{1.0 \text{ mm}}$  in the tension side, because long term holding at elevated temperature is supposed to be applied in the practical design.

In the horizontal welded plate, cracks were detected only in the BM and/or HAZ (Fig.4(a)), and no cracks were observed in the WM. The area where the cracks were generated was assumed to be the HAZ, although it was difficult to distinguish the HAZ from the BM. On the other hand, cracks were observed in both the WM and BM in the longitudinal welded plate (Fig.4(b)). In this case, the cracks in the BM on the compression holding side were initiated at less cycles than in the WM. To verify the results of the plate bending tests, the values of  $N_{1.0 \text{ mm}}$  for uniaxial creep-fatigue tests were obtained (Table 3). The results for uniaxial creep-fatigue tests at strain ranges of 0.5% and 0.7% corresponded to those of the plate bending tests with  $\delta = \pm 3.145$  mm and  $\pm 4.220$  mm, respectively. As observed in the plate bending tests, cracks were initiated less cycles in the BM and/or HAZ with the compression holding test compared to that with the tension holding tests.

Examples of the longest surface cracks (approximately 1.0 mm) are shown in Fig.5, where the cracks are manually colored for visibility. In the horizontal welded plate (Fig.5(a)), the cracks were assumed to be initiated at the boundary between the BM and HAZ, and then propagated along the boundary line.

The results of magnetic particle testing of the specimens subjected to the creep-fatigue tests are shown in Fig.6. In the horizontal welded plate, the cracks propagated along the HAZ on both the compression and tension holding sides. On the tension holding side, cracks along the HAZ line were detected only near the edges on one side of the two HAZ lines. Moreover, slight intrusion was observed at the HAZ line on the tension holding side.

On the compression holding side in the longitudinal welded plate, the cracks appeared to be distributed uniformly in the specimen center, where the maximum strain range was generated at the maximum temperature of 550 °C. Note that the crack density seemed to be relatively large in the WM region. On the tension side in the longitudinal welded plate, most of the cracks were detected in the WM region.

### 3 Evaluation of the test results

#### 3.1 FEA

To evaluate the test results, elastic and inelastic FEAs were performed. The FEA models for the horizontal and longitudinal welded plate specimens are shown in Fig.7. To simulate the tests using the horizontal and longitudinal welded plate specimens, two-dimensional 1/2 sector models and three-dimensional 1/4 sector models were used, respectively. Both elastic and inelastic FEAs were performed using the FINAS code [29]. Here, inelastic FEA means an elastic-plastic-creep FEA, and the four-node quadrilateral plane strain elements QPLAN4 and eight-node hexahedral elements HEX8 of the FINAS code were utilized for the horizontal and longitudinal welded plates, respectively. The jigs were assumed to be rigid bodies, and the temperature distributions measured during the tests were used. To develop a simplified evaluation method using elastic FEA, an analysis model composed of only the BM was used in the elastic FEA.

In the present study, to simulate the metallurgical discontinuities in the weld joints, the model based on the three materials (BM, HAZ, and WM) was applied using the same material properties as those used in Part I (Table 4)[9].

The material properties for the BM were obtained from the JSME FRs code [2] and its background paper [3]. The material properties of the WM were defined based on those of the BM by referring to the previous study [11]. In the previous study, the cyclic stress-strain curve of the WM was adjusted by multiplying the offset yield strength by a factor of 1.1 on the basis of the material testing of the WM [11]. The other properties of the WM that were used were coincident with those of the BM in the JSME FRs code.

The material properties of the HAZ were also defined based on those of the BM in the JSME FRs code; namely, the creep properties of the HAZ were assumed to be those in the JSME FRs code after applying a time factor, ( $\alpha_R$ ), of 10 by referring to the material test result of the



simulated HAZ in Part I [9]. As a result, the creep rupture time of the HAZ was 10 times less than that of the BM. In addition, in the same manner as the Part I [9], the creep-relaxation rate was accelerated because the creep strain equation in the JSME FRs code includes the creep rupture equation with time factor ( $\alpha_R$ ).

To consider the cyclic softening characteristics of Mod.9Cr-1Mo steel, one half of the cyclic stress–strain curve was applied for the FEA. In fact, Mod.9Cr-1Mo steel is gradually softened during cyclic loading, and the application of a kinematic model to express this behavior may be more reasonable. Nevertheless, the important objective in the present study was the development of a method for evaluating the creep-fatigue life of Mod.9Cr-1Mo steel weld joints for use in a design rule, not the simulation of changes in material responses. Therefore, a stable stress–strain response represented by one half of the cyclic stress–strain curve was assumed to be adequate.

### 3.2 Comparison of the FEA and test results

The stress distributions on the surfaces calculated using the FEA are shown in Fig.8. The von Mises equivalent stress was examined in this case.

The results for the horizontal welded plate are shown in Fig.8(a). The value of X-directional stress ( $\sigma_x$ ) was approximately 0, and the ratio of Y-directional stress ( $\sigma_y$ ) to Z-directional stress ( $\sigma_z$ ) was approximately 2.2 and 2.0 before and after holding, respectively (the coordinate system is shown in Fig.7). The maximum stress amplitude was calculated at the boundary between the WM and HAZ before holding, as shown in Fig.8(a). After 1.0 h of holding, stress relaxation led to the redistribution of the stress due to the elastic follow-up caused by the metallurgical discontinuities and creep behavior, resulting in a larger stress at the boundary between the HAZ and the BM and WM.

As shown in Table 4, the stress-strain response used in the FEA was same in the BM and the HAZ; thus the stress amplitude was the same at the boundary between the HAZ and BM before holding. The difference in the stress-strain response between the WM and HAZ resulted in the maximum stress amplitude at the boundary between the WM and HAZ before holding because the offset yield strength of the WM was assumed as 1.1 times larger than that of the BM. On the other hand, the creep strain rate for the HAZ was larger than that of the BM because the time factor ( $\alpha_R$ ) of 10 was applied on the basis of material testing [9], although it was same in the BM and WM. As the result, a larger stress was generated at the boundary between the HAZ and the BM and WM. Namely, the assigned material properties (Table 4), caused the observed stress distribution before and after holding as shown in Fig.8(a).

The stress distribution on the surface in the longitudinal welded plate calculated by FEA is

shown in Fig.8(b). The predicted stress distribution was similar to that of the horizontal welded plate, although the ratios of  $\sigma_y$  to  $\sigma_z$  were approximately 3.0 and 2.3 before and after holding, respectively.

In Part I of this series [9], the evaluation procedure in the JSME FRs code for structural discontinuities was found to be applicable to the evaluation of the strain concentration caused by metallurgical discontinuities in a uniaxial test specimen; namely, the elastic follow-up method described in the JSME FRs code can be used to conservatively estimate the strain concentration and creep damage in the HAZ. The elastic follow-up method was originally developed in Japan, and  $q = 3$  was defined in the code as a conservative value for structural discontinuities.

The elastic follow-up factor  $q$  can be divided into  $q_p$  for elastic-plastic behavior and  $q_c$  for creep-relaxation behavior, although the JSME FRs code does not do so to simplify the rules. The following definitions of the elastic follow-up factor for plastic deformation,  $q_p$ , and creep relaxation,  $q_c$ , were applied [30].

$$q_p = \frac{\Delta \varepsilon_p}{(\Delta \sigma_{el} - \Delta \sigma) / E} \quad (1)$$

$$q_c = \frac{\Delta(\varepsilon_p + \varepsilon_c)}{(\Delta \sigma_{el} - \Delta \sigma) / E} \quad (2)$$

In these equations,  $\Delta \varepsilon_p$  is the plastic strain range calculated by inelastic FEA,  $\Delta \sigma_{el}$  and  $\Delta \sigma$  represent the stress ranges calculated by elastic and inelastic FEA, respectively, and  $E$  is the elastic modulus.  $\Delta(\varepsilon_p + \varepsilon_c)$  is the sum of the plastic and creep strain ranges calculated by inelastic FEA. The elastic follow-up factor was calculated by comparing the results of the elastic and inelastic FEAs [30].

Under operating conditions with low primary stress, the equation for estimating the total strain range,  $\varepsilon_t$ , in the strain concentration region exhibiting elastic follow-up behavior in the JSME FRs code is as follows:

$$\varepsilon_t = K_\varepsilon \varepsilon_n, \quad (3)$$

where  $\varepsilon_n$  is the nominal strain range, and the strain concentration factor,  $K_\varepsilon$ , is defined by the equation in the JSME FRs code as follows:

$$K_{\varepsilon} = KK'_e, \quad (4)$$

where

$$Sn > 3\bar{S}m, \quad (5)$$

$$K'_e = 1 + (q-1)(1 - 3\bar{S}m/Sn), \quad q = 3 \quad (6)$$

$Sn$  is the nominal stress range, and  $K$  is the stress concentration factor. The parameter  $3\bar{S}m$  is the same as that defined in ASME Sec.III Div.1 Subsection NH, Nonmandatory appendices T1324. Note that the value of the strain concentration factor  $K_{\varepsilon}$  is defined as the larger of the calculated value of the modified Neuber's law and the elastic follow-up method in the JSME FRs code. The evaluation steps of equations (3) through (6) indicate a procedure for estimating the strain concentration by the elastic follow-up method.

The results of the FEA rearranged according to these equations using the results of the elastic and inelastic FEAs in the horizontal welded plate are shown in Fig.9(a). In Fig.9(a), the strain concentration factor,  $K_{\varepsilon}$ , calculated from the relationship between inelastic and elastic FEA and that calculated by elastic FEA with elastic follow-up method are shown. In case of using the results of elastic FEA with elastic follow-up method, the JSME FRs code equations with the elastic follow-up factors  $q_p$  of 3.0 and 1.5 were applied. A value of 1.5 for  $q_p$  was applied to take into account the strain concentration of the BM and HAZ. The results calculated in the same manner for the longitudinal welded plate are shown in Fig.9(b). Similarly, comparable strain concentration factors for the BM and HAZ were assumed by applying a  $q_p$  of 1.5 in the elastic FEA.

The accumulated creep damages calculated by inelastic FEA in the BM, HAZ, and WM were also estimated, and the results along with those calculated using the elastic follow-up method described in the JSME FRs code are shown in Fig.10. Namely, the accumulated creep damage calculated using the results of elastic FEA with elastic follow-up factors  $q_c$  of 3.0 and 1.5 are shown in the Fig.10. A  $q_c$  value of 1.5 was applied to take into account the accumulated creep damage in the HAZ.

In Part I of this series [9], the appropriate values for the elastic follow-up factors  $q_p$  and  $q_c$  were both found to be 1.3 for the uniaxial specimen. Therefore, the values for the plate bending test were larger than those for the uniaxial test. The results shown in Fig.9 and Fig.10 revealed that by using  $q_p = q_c = 3$ , large strain concentration factor and accumulated creep damage were calculated for the cyclic bending tests with weld plates.  $K_{\varepsilon}$  values calculated by inelastic FEA in the BM and HAZ were comparable to those obtained by applying  $q_p = 1.5$  in

the elastic follow-up method. Similarly, the creep damages calculated by inelastic FEA in the BM and HAZ were estimated to be comparable by applying a value of  $q_c = 1.5$  in the elastic follow-up method. These results indicated that this simplified technique for estimating the strain concentration and accumulated creep damage in structural discontinuities based on the elastic follow-up method is applicable to evaluate the metallurgical discontinuities in Mod.9Cr-1Mo steel weld joints, however, the value of the elastic follow-up factor defined in the JSME FRs code for structural discontinuities overestimates the strain concentration and accumulated creep damage in the weld joints. Therefore, for cyclic bending tests using weld joints, a conservative value of 1.5 is recommended for both the elastic follow-up factors  $q_p$  and  $q_c$ .

### 3.3 Proposed simplified evaluation method

The evaluation of the creep-fatigue life using inelastic FEA was proposed in Part I [9]. In Part I, the creep-fatigue life was estimated at each location in the BM, HAZ, and WM where the maximum stress was generated [9]. Namely, the material properties of the BM, HAZ and WM were used to estimate the creep-fatigue life at each location, and the minimum number of cycles to failure for the three regions was assumed to be the failure cycle for the weld joint. To estimate the number of cycles to failure, creep-fatigue damage was estimated based on the linear accumulative damage rule, where the accumulative fatigue damage ( $D_f$ ) and accumulative creep damage ( $D_c$ ) are evaluated individually. As a failure criterion under the superposition of creep and fatigue damages, a bilinear criterion ( $D_f, D_c$ ) is applied such that  $(D_f, D_c) = (1, 0)$ ,  $(0.3, 0.3)$ , and  $(0, 1)$ , because the applicability of this bilinear criterion,  $(D_f, D_c) = (1, 0)$ ,  $(0.3, 0.3)$ , and  $(0, 1)$ , for the structural testing of Mod.9Cr-1Mo steel with inelastic FEA using one half of the cyclic stress–strain curve was previously confirmed[12].

While inelastic FEA is a useful tool, it is costly to design all of the necessary components. Therefore, a procedure using elastic FEA with a simplified technique for evaluating the creep-fatigue damage in the weld joints is required for codification, because inelastic FEA including the modeling of the weld lines in components is not practical for actual component design. In the actual design, creep-fatigue damage is calculated from the results of an elastic analysis using a simplified technique. In other words, the inelastic behavior of the material at structural discontinuities in components is estimated from the results of elastic analysis in the ordinary design codes, and a simplified evaluation procedure using elastic FEA for Mod.9Cr-1Mo steel weld joints is required for codification. Therefore, a simplified technique has been proposed, and is summarized in Fig.11.

Many variations in weld joints (e.g., differences in the chemical composition of the WM, weld conditions, and groove configurations) should be considered. Therefore, the evaluation method for establishing design rules must be robust and should have an application scope. To

ensure the robustness of the proposed method, additional procedures were considered in the calculation of fatigue and creep damage (Fig.11).

Since, the proposed procedure evaluates metallurgical discontinuities due to welding by using the elastic follow-up method developed for estimating structural discontinuities, an FEA model based on the BM properties is used for this proposed procedure. An elastic FEA is performed, and the total strain range ( $\varepsilon_t$ ) is then calculated by combining the nominal stress range and the elastic follow-up method.

The calculated results shown in Fig.9, Fig.10, and Part I (for uniaxial tests) indicate that the evaluation procedure based on the elastic follow-up method with  $q_p = q_c = 1.5$  enables the conservative estimation of the strain range concentration and accumulated creep damage due to metallurgical discontinuities [9]. In other words, the elastic follow-up method developed for estimating the strain concentration at structural discontinuities is applicable to evaluate the metallurgical discontinuities of Mod.9Cr-1Mo steel weld joints using an appropriate elastic follow-up factor. Therefore, in this proposed procedure,  $q_p = q_c = 1.5$  are applied as an recommended value.

In the evaluation of fatigue damage, the calculated  $\varepsilon_t$  is multiplied by a  $K_f$  of 1.1 to calculate the fatigue damage caused by the nominal fatigue curve of the BM. Because failure is assumed to occur at the WM in the high cycle fatigue region with lower creep-damage conditions, a fatigue reduction factor,  $K_f$ , of 1.1 should be applied. The value of 1.1 was defined based on the results of the fatigue tests for the WM [11].

In the evaluation of creep damage, the initial relaxation stress is also estimated from a combination of the  $\varepsilon_t$  value and tensile curve. Namely, the initial stress is defined as corresponding to the monotonic strain–strain curve to  $1/2 \times \varepsilon_t$  for the conservative estimation of the creep damage, which is the same approach as that used in the JSME FRs code [3]. In this proposed procedure, the creep damage during relaxation is estimated by using the creep rupture curve for weld joints [6]. In other words, the creep strength is decreased in the proposed procedure by using the creep rupture curve for weld joints [6] because of the variations in the material properties of the HAZ due to the welding conditions, and the ratio of the HAZ width to the overall size of the vessel and piping is supposed to be significantly smaller than that of the test specimens applied in the series study. Using the creep rupture curve of the weld joint [6] is expected to account for the variation in material properties and HAZ configuration.

These implicitly applied conservative evaluation procedures were then superimposed on the design factors. As a result, the evaluation procedure proposed in Fig.11 is believed to be very robust.

### 3.4 Evaluated results

A comparison of the experimentally determined number of cycles and the estimated failure cycles for the horizontal welded plate is shown in Fig.12 and Fig.13, where the  $N_{25\% \text{ drop}}$  and  $N_{1.0 \text{ mm}}$  in the compression and tension holding sides are indicated.

The estimated cycles were calculated from the inelastic analysis based on the model with the three materials and by using the procedure proposed in Fig.11. The evaluation using the inelastic analysis was performed as described in Part I [9]. Namely, the failure cycles were estimated in the BM, HAZ and WM at the integral points where the maximum stress was generated on the surface; then, the minimum number of cycles and its location were assumed to be the failure cycle and failure location of the weld joint. In this estimation, the creep rupture time of the HAZ was assumed to be 1/10 for the creep damage calculation and the strain range of the WM was multiplied by 1.1 for the fatigue damage calculation. Two results calculated by the procedure described in Fig.11 are also shown in Fig.12 and Fig.13. One was obtained directly with nominal creep rupture and fatigue failure equations, and the second was calculated using the design factors and additional conservative procedures described in the JSME FRs code with the proposed procedure [4].

The fatigue test results and estimated failure lives for the horizontal welded plate are compared in Fig.12. When failure was estimated using  $N_{1.0 \text{ mm}}$ , the predicted values were within a factor of 3 for both  $\delta = \pm 3.145 \text{ mm}$  and  $4.220 \text{ mm}$  when compared with the values obtained by inelastic FEA. On the other hand, the results estimated using the proposed procedure (Fig.11) without the design factors were comparable to those obtained by inelastic FEA. The results estimated using the proposed procedure (Fig.11) with the design factors described in the JSME FRs code were within a factor of 20 when these compared with  $N_{1.0 \text{ mm}}$ .

The creep-fatigue test results and estimated failure lives for the in horizontal welded plate are compared in Fig.13. Similar results were obtained in the fatigue and the creep-fatigue test; however, the values predicted in the creep-fatigue test were more conservative than those obtained in the fatigue test. The minimum number of cycles to failure calculated by inelastic FEA was determined at the HAZ. Therefore, the number of failure cycles predicted by inelastic FEA was defined based on the estimated failure cycle of the HAZ in the creep-fatigue test, and this result agreed with the experimental results shown in Fig.4(a), Fig.5(a), and Fig.6. When failure was estimated using the  $N_{1.0 \text{ mm}}$  on the tension holding side, the predicted values were within a factor of 5 compared with the values obtained by inelastic FEA for both  $\delta = \pm 3.145 \text{ mm}$  and  $4.220 \text{ mm}$ . When failure was assumed to  $N_{1.0 \text{ mm}}$  on the compression holding side, the predicted values were within a factor of 3. The estimated results using the proposed procedure (Fig.11) without the design factors were comparable with those obtained by inelastic FEA. The results estimated using the proposed procedure (Fig.11) with the design factors described in the

JSME FRs code were within a factor of 200 when these compared with  $N_{1.0\text{ mm}}$  of the tension holding side. This level of conservativeness is comparable with that of values estimated for the BM using other structural tests performed to confirm the design margins for the creep-fatigue evaluation procedure of Mod.9Cr-1Mo steel in the JSME FRs code [3].

The estimated results for the longitudinal welded plate were also compared with the experimental results obtained in the cyclic bending tests (Fig.14 and Fig.15). As in Fig.12 and Fig.13, three distinct numbers of cycles are indicated in Fig.14 and Fig.15. The results for the longitudinal welded plate were similar to those for the horizontal welded plate. The failure cycles predicted by inelastic FEA was defined based on the estimated failure cycles of the WM in the creep-fatigue test, and was comparable to the BM and HAZ. As with the horizontal welded plate, this result agreed with the experimental results shown in Fig.4(b), Fig.5(b), and Fig.6. In the case of the creep-fatigue test shown in Fig.15, when  $N_{1.0\text{ mm}}$  of the tension holding side is applied, the predicted values were within a factor of 5 compared with the values obtained by inelastic FEA for both  $\delta = \pm 3.145\text{ mm}$  and  $4.220\text{ mm}$ , and these values were also comparable to the results obtained using the proposed procedure (Fig.11) without the design factors. The results obtained using the procedure outlined in Fig.11 and the design factors described in the JSME FRs code were within a factor of 325 when  $N_{1.0\text{ mm}}$  of the tension side was applied. This level of conservativeness is comparable with that of the values estimated for the BM [3].

Overall, these results indicate that the proposed simplified procedure (Fig.11) is applicable as a design method. Because it is based on a procedure for evaluating the creep-fatigue life of structural discontinuities and modified for evaluating that of metallurgical discontinuities in the weld joint, the proposed procedure is harmonized with the conventional procedure for evaluating creep-fatigue damage. In fact, the applicability of the proposed procedure, which is based on elastic FEA using a simplified technique, as an evaluation procedure for the JSME FRs code was confirmed in this study. Moreover, the failure cycles estimated using the proposed procedure were demonstrated to be comparable to the design margin for structural discontinuities subject to cyclic loading accompanied by creep-fatigue damage.

This proposed procedure is based on the test results for a tungsten inert gas (TIG) weld with full penetration. Therefore, the scope of the application may be limited to TIG welds with full penetration. Clearly, weld locations where both metallurgical and structural discontinuities are superimposed are also beyond the scope of this method. On the other hand, the recommended value of 1.5 for  $q_p$  and  $q_c$  was defined based on the results of both uniaxial and plate bending tests. Therefore, the optimized value for codification may be defined using the results by inelastic FEA based on various models and loading conditions for conceivable component weld lines. If elastic follow-up factors larger than 1.5 were confirmed in these studies, larger values

should be redefined. In this paper, the main proposal is that the approach to evaluate structural discontinuities can be applicable to the metallurgical discontinuities in the weld joint. Therefore, to validate the applicability, long term holding tests, tests at 600 °C (accelerated temperature tests) and other structural tests are required for codification in addition to FEA.

#### 4 Conclusions

Plate bending fatigue and creep-fatigue tests for Mod.9Cr-1Mo steel weld joints were performed as structural tests. To apply the failure criterion of a crack appeared on the surface with a length of 1.0 mm,  $N_{1.0mm}$ , the tests were interrupted several times to collect replicas of the surface in order to observe crack initiation and propagation. Moreover, a simplified estimation procedure using elastic FEA with the elastic follow-up method was proposed based on the elastic and inelastic FEA results, and the creep-fatigue life was evaluated using the proposed procedure based on elastic FEA and the procedure described in Part I of this series based on inelastic FEA [9]. These results and experimentally obtained  $N_{1.0mm}$  were then compared.

- (1) Creep-fatigue lives estimated by the proposed procedure based on the elastic FEA and a simplified technique were comparable with those estimated by inelastic FEA.
- (2) The estimated creep-fatigue lives based on inelastic FEA predicted the experimentally obtained  $N_{1.0mm}$  within a factor of 5 for all creep-fatigue plate bending tests.
- (3) The applicability of the proposed procedure, which is based on elastic FEA using a simplified technique, as an evaluation procedure for the JSME FRs code was confirmed.

#### Acknowledgement

This study includes results for the “Technical development program on a commercialized FBR plant” entrusted to the Japan Atomic Energy Agency (JAEA) by the Ministry of Economy, Trade, and Industry of Japan (METI). The authors are grateful to Mr. Yasuhiko Inoue of ASEND, Ltd. for performing the FEA.

#### References

- [1] Aoto, K., Uto, N., Sakamoto, Y., Ito, T., Toda, M., Kotake, S. 2011. Design Study and R&D Progress on Japan Sodium-Cooled Fast Reactor. Journal of Nuclear Science and Technology 2011, Vol.48, pp.463-471
- [2] Japan Society of Mechanical Engineers: Codes for Nuclear Power Generation Facilities, Rules on Design and Construction for Nuclear Power Plants, Section II Fast Reactor Standards, 2012, JSME S NC2-2012 (in Japanese)
- [3] Ando, M., Watanabe, S., Kikuchi, K., Otani, T., Satoh, K., Tsukimori, K., Asayama, T. Development of 2012 Edition of JSME Code for Design and Construction of Fast Reactors



- (6) Design margin assessment for the new materials to the rules PVP2013-97803, Proceedings of the ASME 2013 Pressure Vessels and Piping Conference
- [4] Iida, K., Asada, Y., Okabayashi, K., Nagata, T. Construction codes developed for prototype FBR Monju. Nucl. Eng. Des. 1987, 98, 283–288.
- [5] Iida, K., Asada, Y., Okabayashi, K., Nagata, T. Simplified analysis and design for elevated temperature components of Monju. Nucl. Eng. Des. 1987, 98, 305–317.
- [6] Wakai, T. Onizawa, T. Kato, T. Date, S. Kikuchi, K. Satoh, K. A study for proposal of welded joint strength reduction factors of modified 9Cr-1Mo steel for Japan sodium cooled fast reactor (JSFR), Proceedings of the ASME 2013 Pressure Vessels and Piping Conference, 2013, PVP2013-97091
- [7] Kimura, K. Creep strength assessment and review of allowable tensile stress of creep strength enhanced ferritic steels in Japan, Proceedings of the ASME 2005 Pressure Vessels and Piping Conference, 2005, PVP2005-71039
- [8] Kimura, K. Assessment of long-term creep strength and review of allowable stress of high Cr ferritic creep resistant steels, Proceedings of the ASME 2006 Pressure Vessels and Piping Conference, 2006, PVP2006-ICPVT-11-93294
- [9] Ando, M., Takaya, S., “Creep-fatigue evaluation method for weld joints of Mod.9Cr-1Mo steel Part I: Proposal of the evaluation method based on finite element analysis and uniaxial testing ” Nucl. Eng. Des. *[Submitted]*
- [10] Kato, S., Furukawa, T. and Yoshida, E., 2008, “Material Test Data of Mod.9Cr-1Mo steel (1),” JAEA-Data/Code 2008-030, in Japanese.
- [11] Takaya, S. Evaluation of fatigue strength of similar and dissimilar welded joints of modified 9Cr-1Mo steel, Proceedings of the 22th international conference on nuclear engineering, ICONE22-30022
- [12] Ando, M., Hirose, Y., Karato, T., Watanabe, S., Inoue, O., Kawasaki, N., Enuma, Y. “Comparison and assessment of the creep-fatigue evaluation methods with notched specimens made of Mod.9Cr-1Mo steel,” Journal of Pressure Vessel Technology, Volume 136, Issue 4, p.041406\_1 - 041406\_10
- [13] Ando, M., Kanasaki, H., Date, S., Kikuchi, K., Sato, K., Takasho, H., Tsukimori, K. A study on fatigue and creep-fatigue life assessment using cyclic thermal tests with Mod.9Cr-1Mo steel structures, Proceedings of ASME Pressure Vessel and Piping Conference 2012, 2012, PVP2011-78042
- [14] Ando, M., Hasebe, S., Kobayashi, S., Kasahara, N., Toyoshi, A., Ohmae, T., Enuma, Y. Thermal transient test and strength evaluation of a thick cylinder model made of Mod.9Cr-1Mo steel, Journal of Nuclear Engineering and Design, 2013, No.255, pp.296-309

- [15] Yamauchi M. Igari, T. Matsubara, T. Setoguchi, K. Creep-Fatigue Life Prediction for Modified 9Cr-1Mo Steel by Linear Damage Rule, *Journal of the Society of Materials Science, Japan*, 1990, Vol.39, No.442, pp.965-969 (in Japanese)
- [16] Aoto K. Komine, R. Ueno, F. Kawasaki, H. Wada,Y., Creep-fatigue evaluation of normalized and tempered Modified 9Cr- 1Mo, *Journal of Nuclear Engineering and Design*, 1994, No.153, pp.97-110
- [17] Taguchi, K. Ueta, M. Dozaki, K. Sukekawa, Y. Kato, H. Asada, Y. Creep-fatigue life prediction for Modified 9Cr-1Mo steel, *Proceedings of ASME PVP 1993*, 1993, PVP-Vol. 262, pp.175-180
- [18] Yaguchi, M. Okamoto, Y. Nakamura, T. Asada, Y. Creep-Fatigue Interaction of Modified 9Cr-1Mo Steel in a Very High Vacuum Environment and Experimental Analysis of Overstress, *JSME international journal. Ser. A, Mechanics and material engineering A*, Vol.38, No.2, 1995, pp.220-225
- [19] Yaguchi, M. Nakamura, T. Ishikawa, A. Asada, Y. Creep-fatigue damage assessment by subsequent fatigue straining,” *Nuclear Engineering and Design*, Vol.162, 1996, pp.97-106
- [20] Yukio T. Study on creep-fatigue evaluation procedures for high-chromium steels—Part I: Test results and life prediction based on measured stress relaxation, *International Journal of Pressure Vessels and Piping*, 2008, Vol. 85, pp.406-422
- [21] Kobayashi, K. Hayakawa, M. Kimura, M. Yamaguchi, K. Effects of compressive strain hold on low-cycle fatigue life at elevated temperatures, *Strength, fracture and complexity*, Vol. 5, No.2-3, 2009, pp. 89-96
- [22]Fournier, B. Sauzay, M. Caës, C. Noblecout, M. Mottot, M. Bougault, A. Rabeau, V. Pineau, A. Creep-fatigue–oxidation interactions in a 9Cr–1Mo martensitic steel. Part I: Effect of tensile holding period on fatigue lifetime, *International Journal of Fatigue*, Vol.30, 2008, pp.649-662
- [23]Fournier, B. Sauzay, M. Caës, C. Noblecout, M. Mottot, M. Bougault, A. Rabeau, V. Pineau, A. Creep-fatigue–oxidation interactions in a 9Cr–1Mo martensitic steel. Part II: Effect of compressive holding period on fatigue lifetime, *International Journal of Fatigue*, Vol.30, 2008, pp.1797-1812
- [24] Fournier, B. Sauzay, M. Caës, C. Noblecout, M. Mottot, M. Bougault, A. Rabeau, Man, J. Gillia, O. Lemoine, P. Pineau, A. Creep-fatigue–oxidation interactions in a 9Cr–1Mo martensitic steel. Part III: Lifetime prediction,” *International Journal of Fatigue*, Vol.30, 2008, pp.663-676
- [25] Shankar V, Valsan, M. Rao, K. Kannan, R. Mannan, L.S. Pathak, D.S. Low cycle fatigue behavior and microstructural evolution of modified 9Cr–1Mo ferritic steel, *Materials Science and Engineering: A*, Vol.437, Issue 2, 2006, pp 413-422

- [26] Kannan, R. Sandhya, R. Ganesan, V. Valsan, M. Rao, K. Effect of sodium environment on the low cycle fatigue properties of modified 9Cr-1Mo ferritic martensitic steel, Journal of Nuclear Materials, No.384, 2009, pp.286-291
- [27] Kannan, R. Ganesan, V. Mariappan, K. Sukumaran, G. Sandhya, R. Mathew, D.M. Bhanu, K. Rao, S. Influence of dynamic sodium environment on creep-fatigue behavior of Modified 9Cr-1Mo ferritic-martensitic steel, Journal of Nuclear Engineering and Design, No.241, 2011, pp.2807-2812
- [28] Nonaka, I. Kitagawa, M. Ohtomo, A. Wada, Y. Effect of compressive strain holding on the low cycle fatigue strength of 21/4Cr-1Mo steel at elevated temperatures, Tetsu-to-Hagane (Journal of Iron Steel Inst. Japan), Vol.73, No.16, 1987, pp.2267-2274(in Japanese)
- [29] Japan Atomic energy agency and Itochu Techno-Solutions, 2008, FINAS User's Manual Ver.19.0, (in Japanese)
- [30] Kasahara, N., Nagata, T., Iwata, K., Negishi, H. Advanced creep-fatigue evaluation rule for fast breeder reactor components: generalization of elastic follow-up model. Nuclear Engineering and Design, Vol. 155, pp.499-518, 1995

## List of figures

Fig.1 Results of the Vickers hardness tests

Fig.2 Configurations of the specimens

Fig.3 Schematic of the plate bending test

Fig.4 Longest surface cracks observed during the bending test with  $\delta = \pm 3.145$  and a holding time of 1 h for the (a) horizontal welded plate and (b) longitudinal welded plate

Fig.5 Crack situation after representative cycles for the bending test with  $\delta = \pm 3.145$  and a holding time of 1 h for the (a) horizontal welded plate and (b) longitudinal welded plate

Fig.6 Magnetic particle testing results for the (a) horizontal welded plate and (b) longitudinal welded plate after creep-fatigue testing with  $\delta = \pm 3.145$  and a holding time of 1 h

Fig.7 Finite element models for the (a) horizontal welded plate and (b) longitudinal welded plate

Fig.8 Stress distribution on the surface of the compression holding side of the (a) horizontal welded plate and (b) longitudinal welded plate

Fig.9 Estimated strain concentration factors for the (a) horizontal welded plate and (b) longitudinal welded plate

Fig.10 Estimated accumulated creep damages in the (a) horizontal welded plate and (b) longitudinal welded plate

Fig.11 Simplified creep-fatigue damage evaluation method for similar Mod.9Cr-1Mo steel weld joints

Fig.12 Comparison of the fatigue test results and estimated failure lives in the horizontal welded plate with (a)  $\delta = \pm 3.145$  mm and (b)  $\delta = \pm 4.220$  mm

Fig.13 Comparison of the creep-fatigue test results and estimated failure lives in the horizontal welded plate with (a)  $\delta = \pm 3.145$  mm and holding for 1 h and (b)  $\delta = \pm 4.220$  mm and holding for 0.5 h

Fig.14 Comparison of the fatigue test results and estimated failure lives in the longitudinal welded plate with (a)  $\delta = \pm 3.145$  mm and (b)  $\delta = \pm 4.220$  mm

Fig.15 Comparison of the creep-fatigue test results and estimated failure lives in the longitudinal welded plate with (a)  $\delta = \pm 3.145$  mm and holding for 1 h and (b)  $\delta = \pm 4.220$  mm and holding for 0.5 h

Fig.1

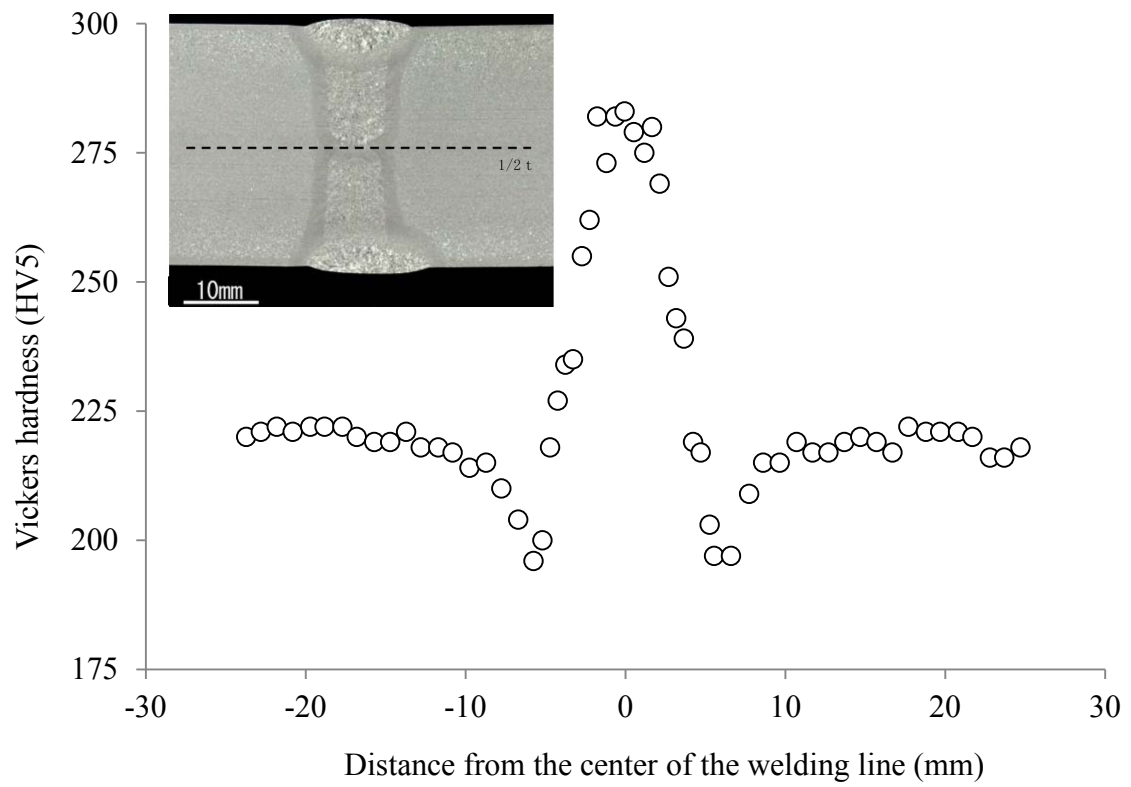


Fig.2

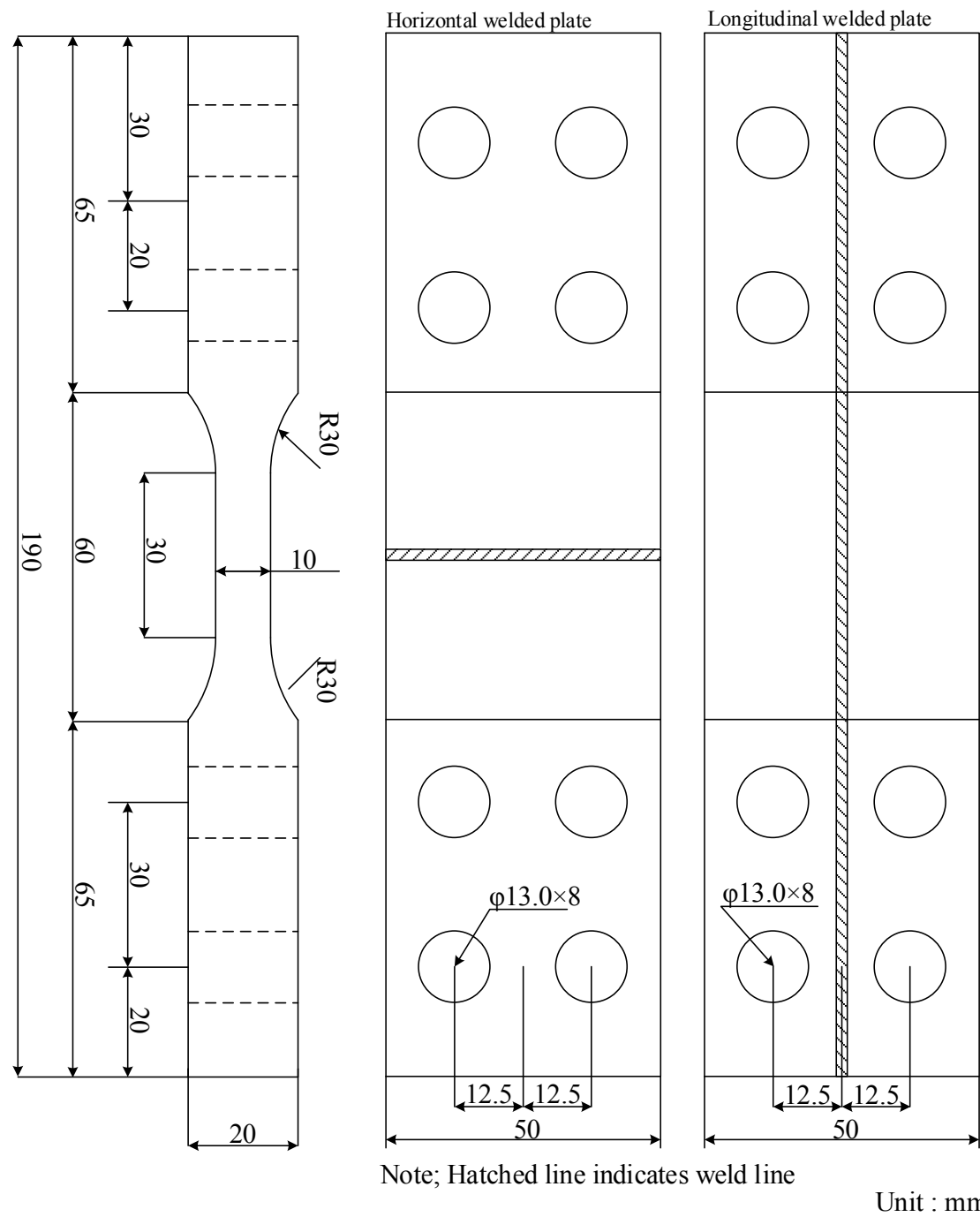


Fig.3

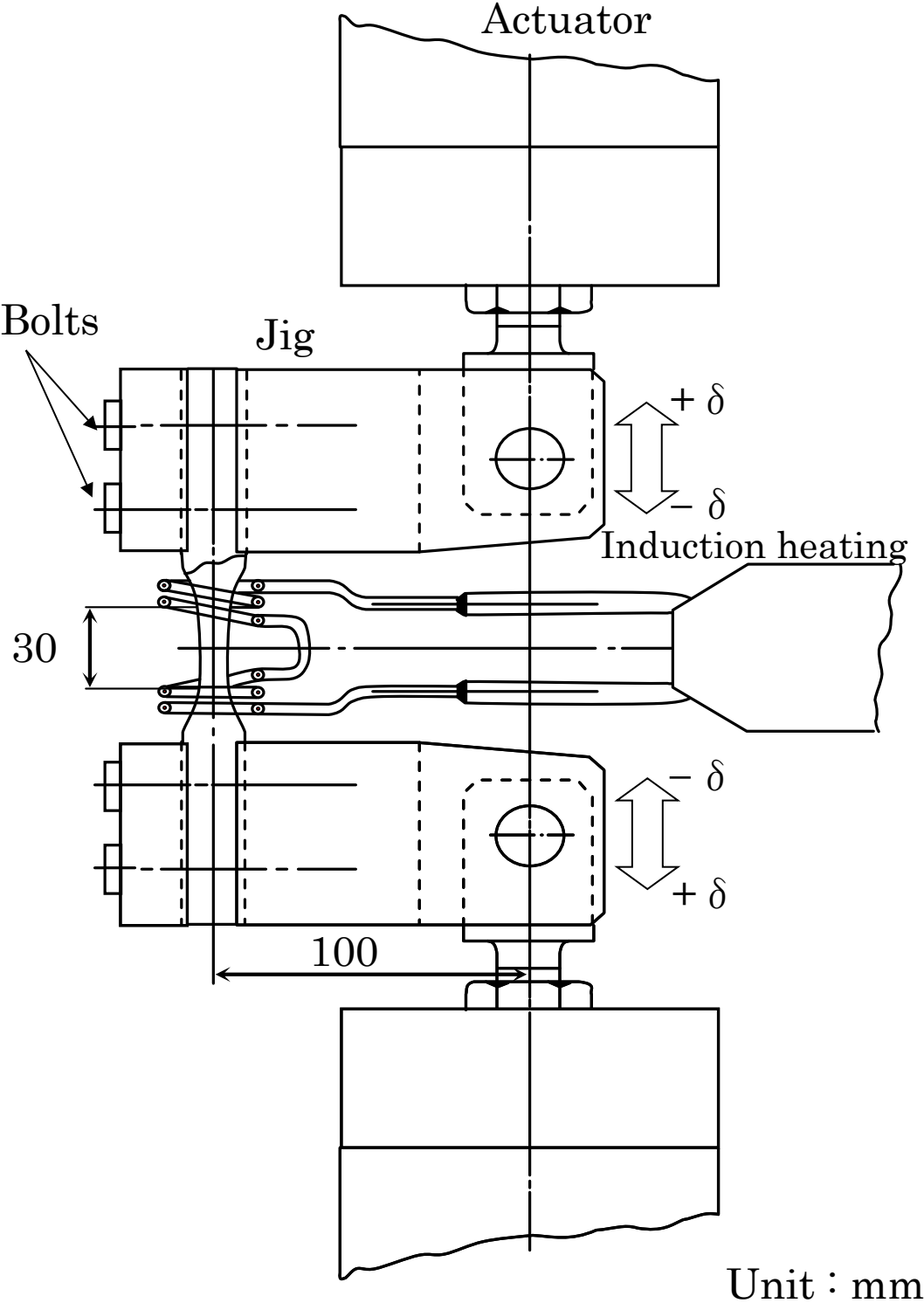


Fig.4

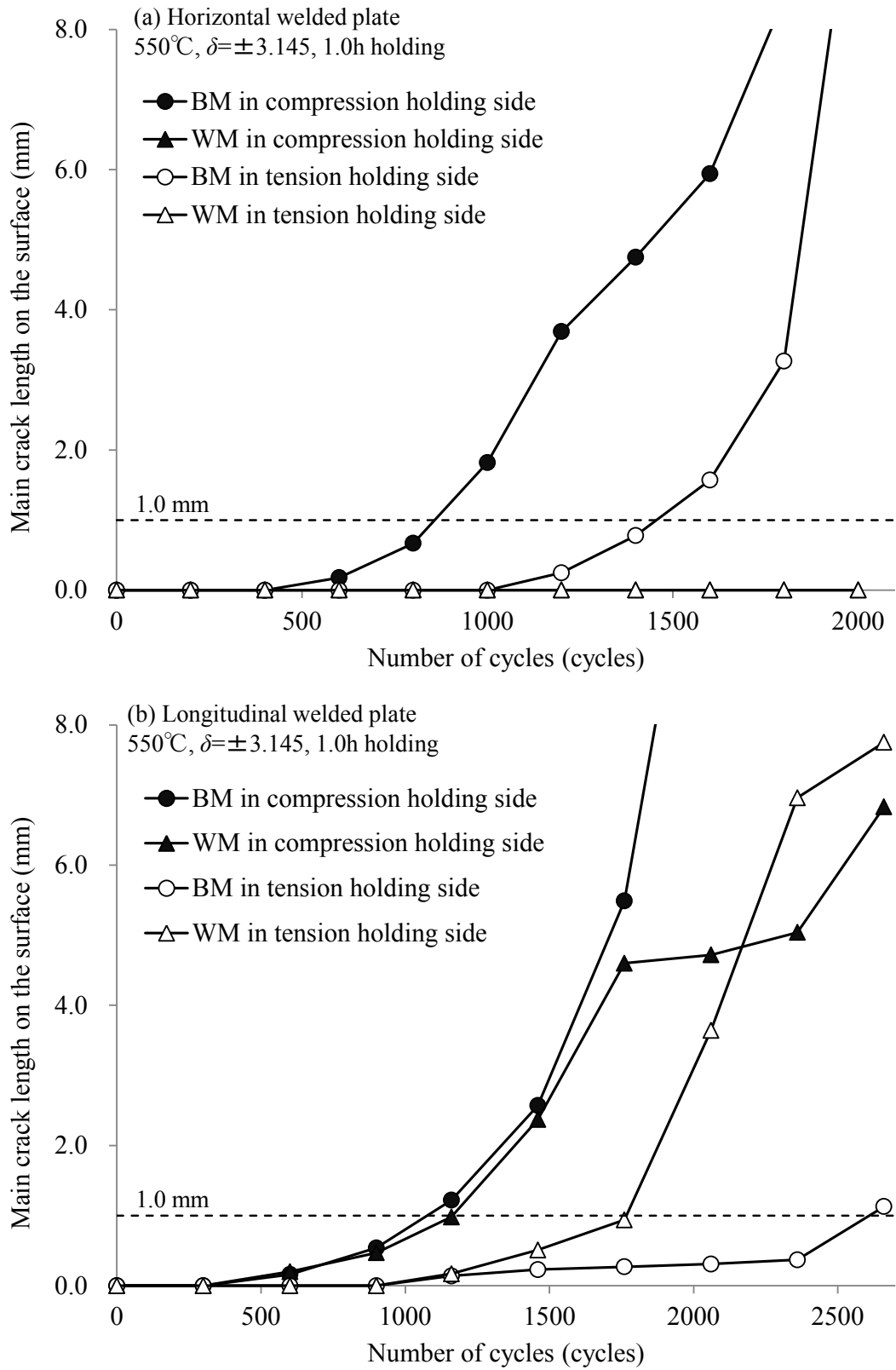




Fig.5

(a)Horizontal welded plate

550°C,  $\delta = \pm 3.145$  mm, 1 h holding, 1160 cycles



(b)Longitudinal welded plate

550°C,  $\delta = \pm 3.145$  mm, 1 h holding, 1000 cycles

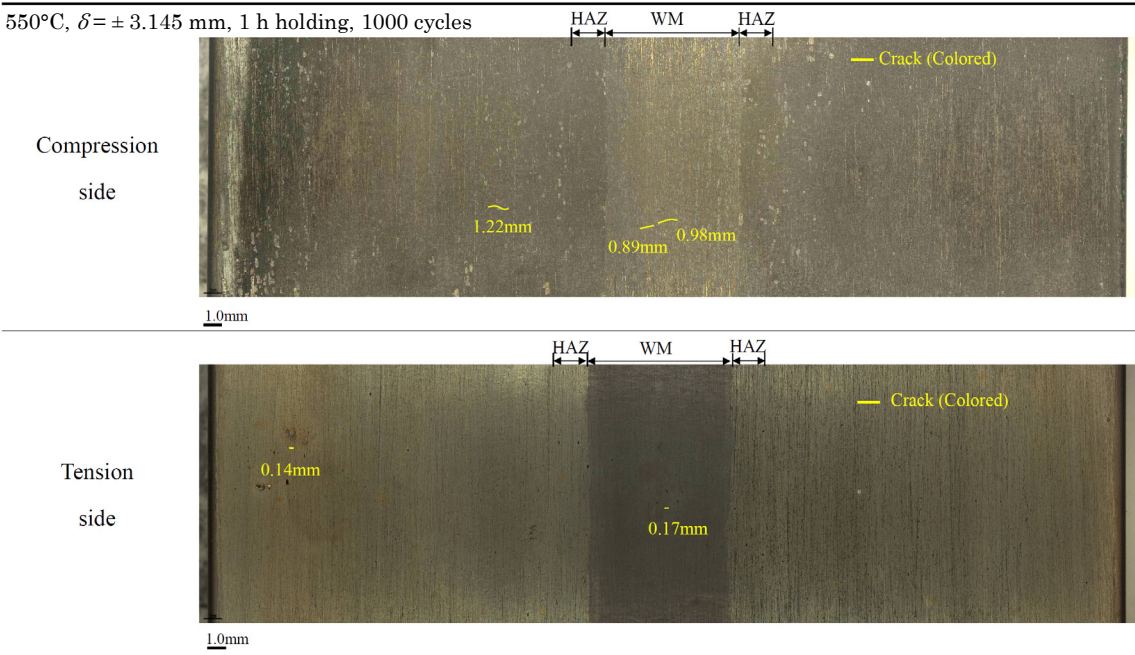


Fig.6

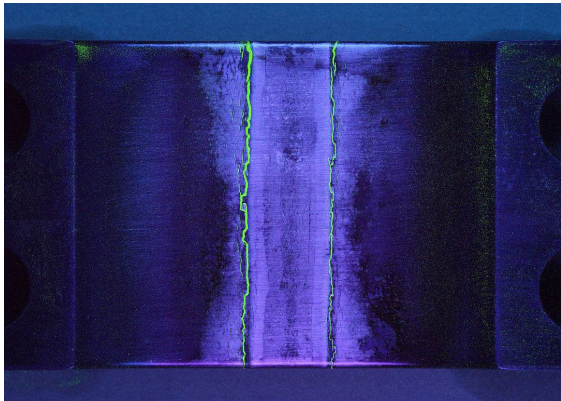
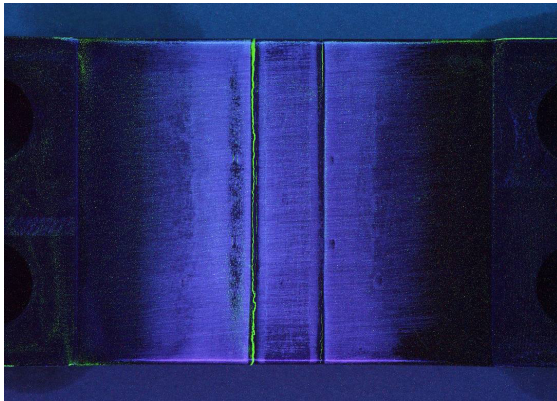
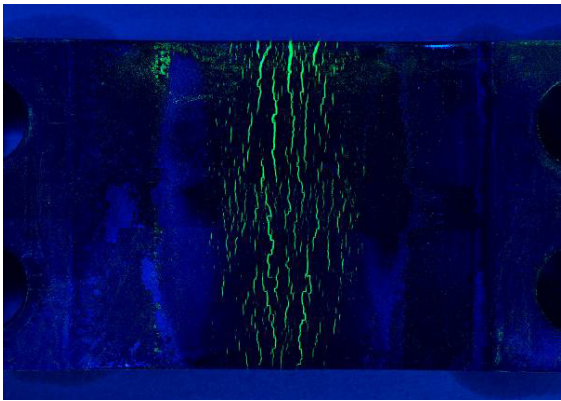
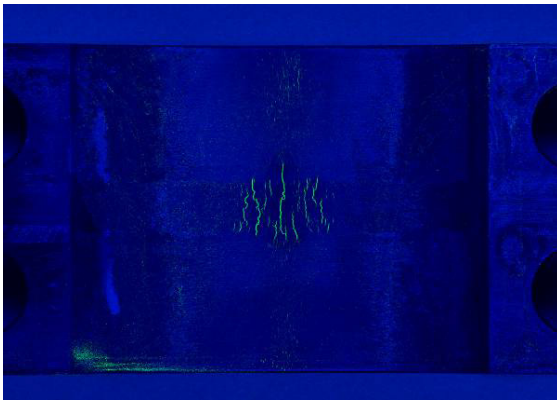
Specimen	Compression holding side	Tension holding side
<p>Horizontal welded plate</p> <p>550°C  <math>\delta = \pm 3.145</math> mm,  1 h holding,  1160 cycles</p>		
<p>Longitudinal welded plate</p> <p>550°C  <math>\delta = \pm 3.145</math> mm,  1 h holding  2650 cycles</p>		

Fig.7

(a)FEA model for the horizontal welded plate

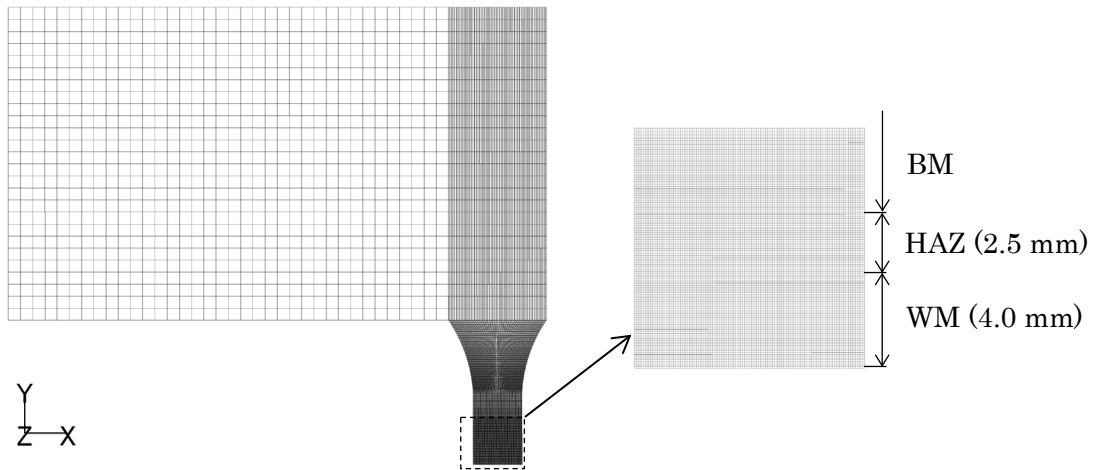


Fig.7

(b)FEA model for longitudinal welded plate

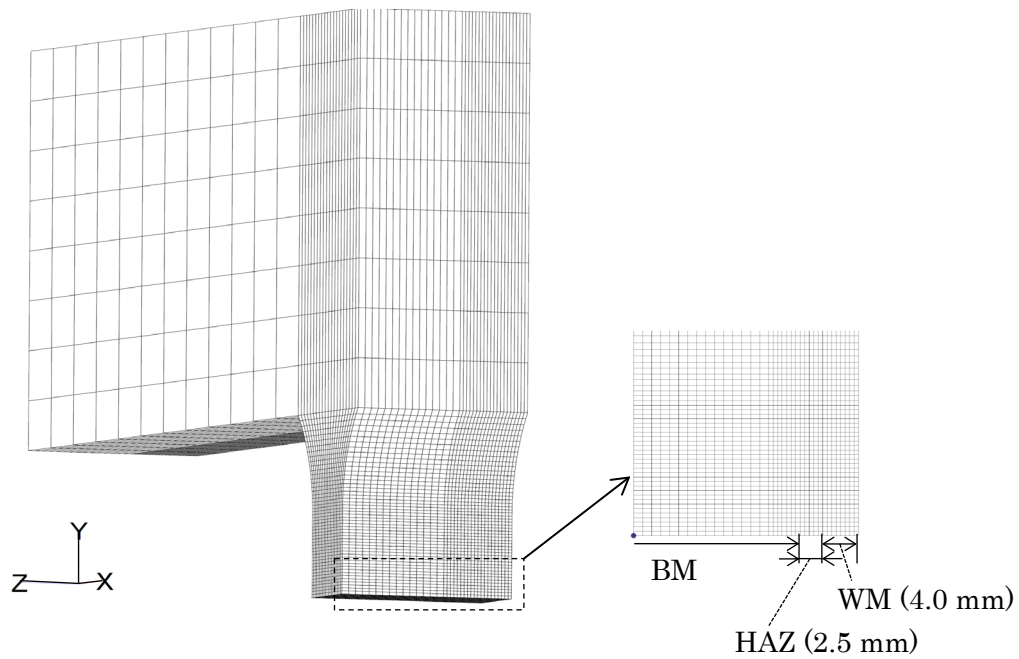


Fig.8

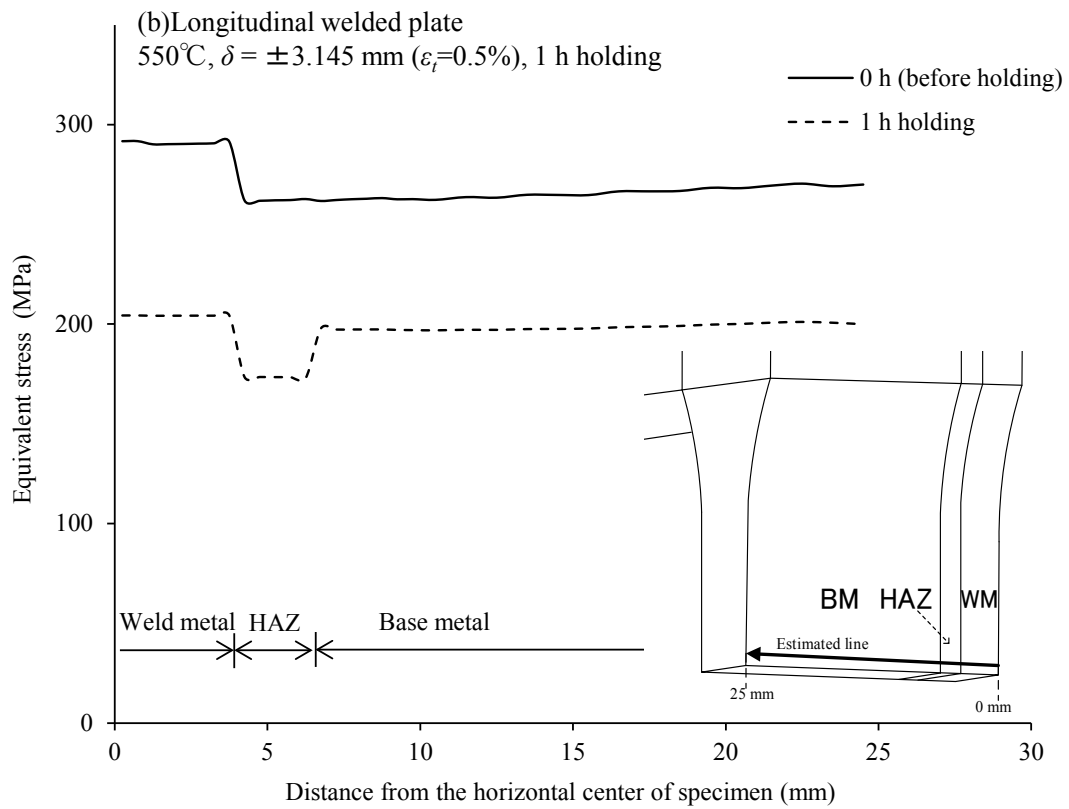
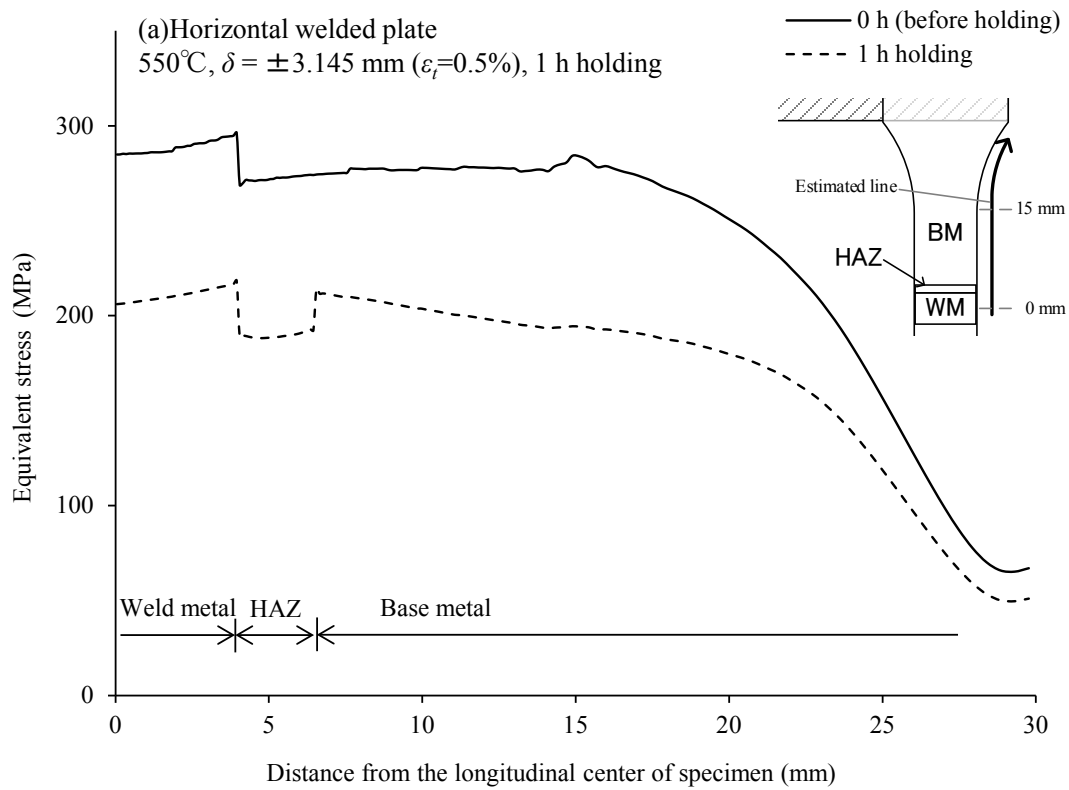


Fig.9

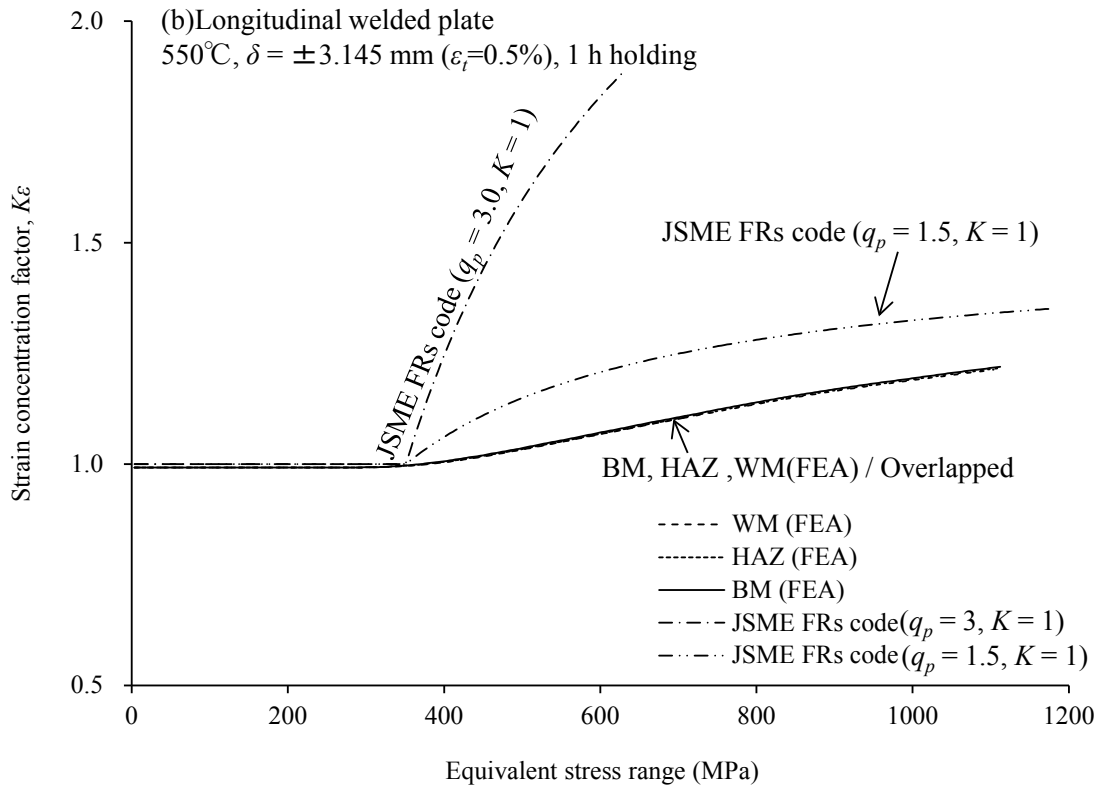
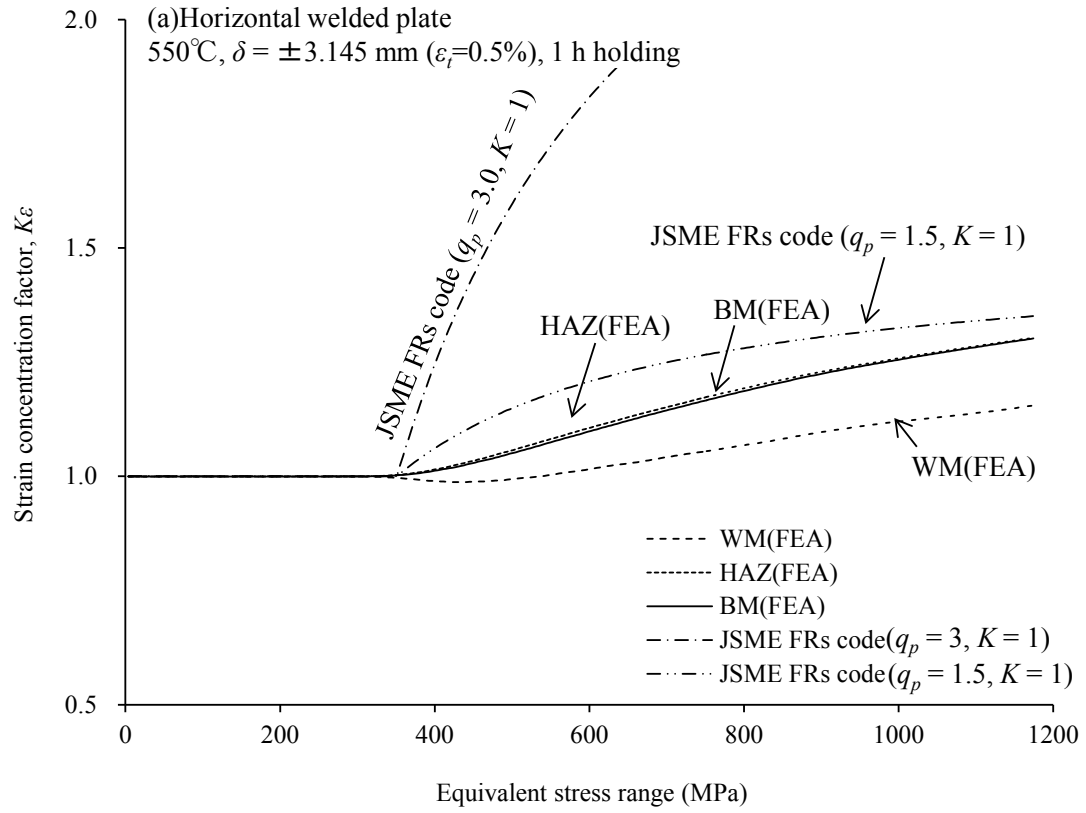


Fig.10

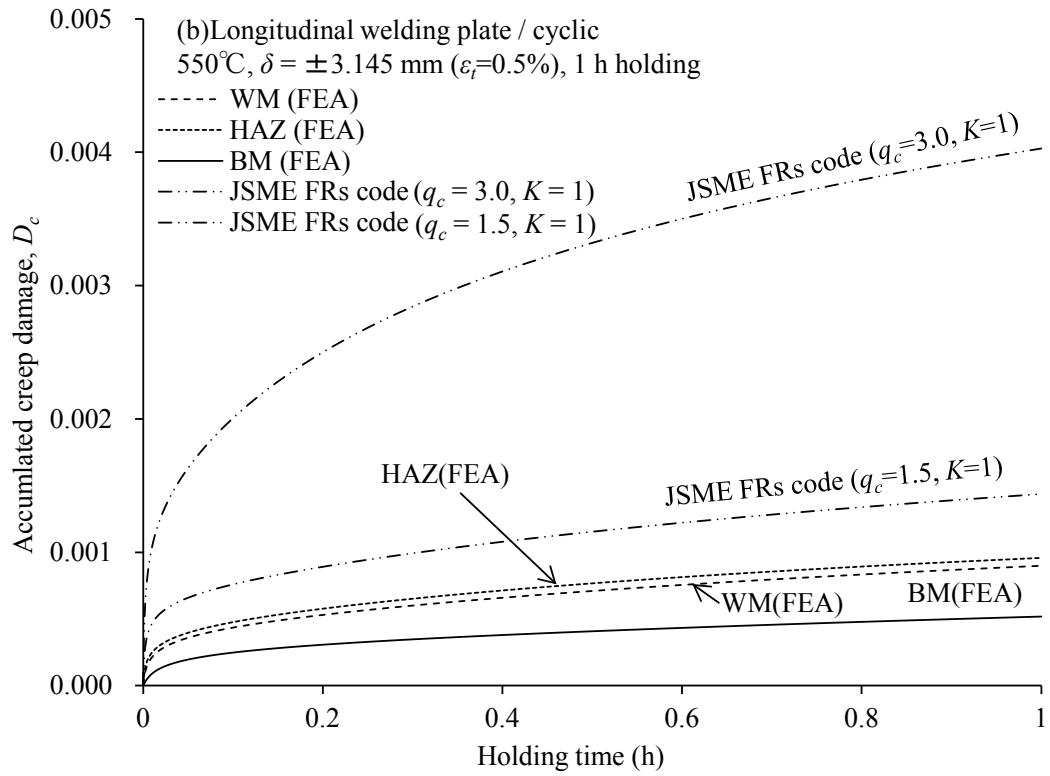
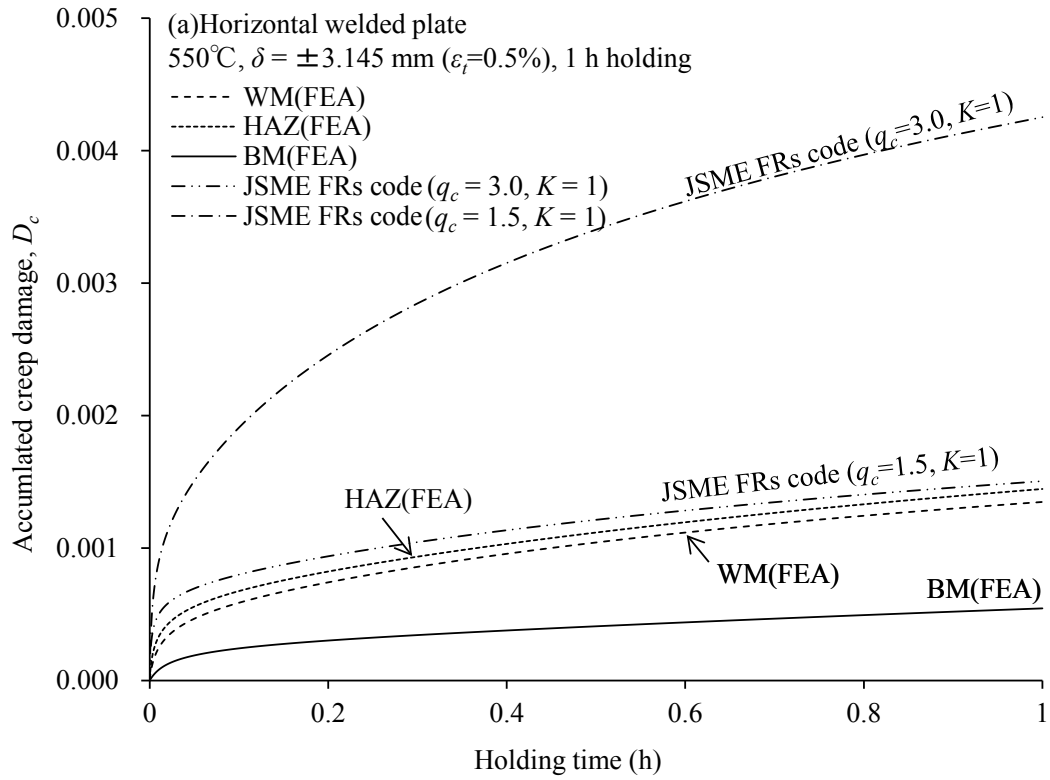


Fig.11

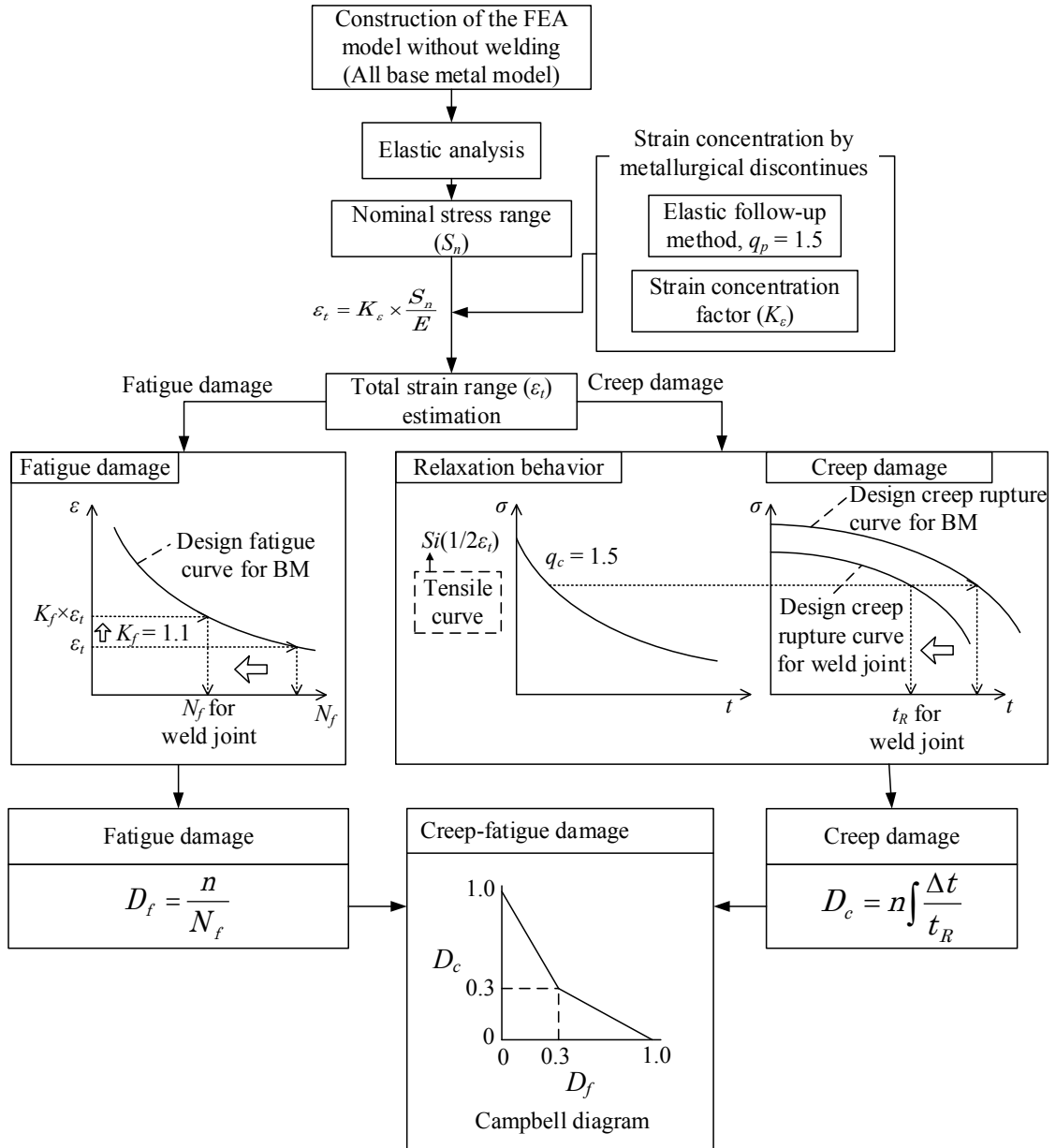


Fig.12

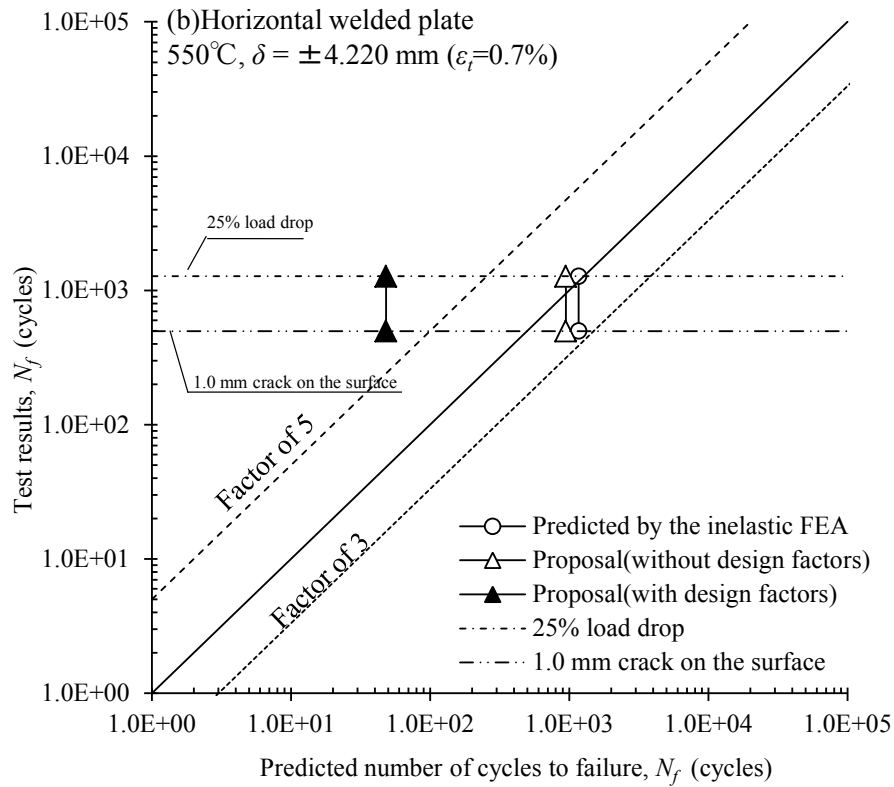
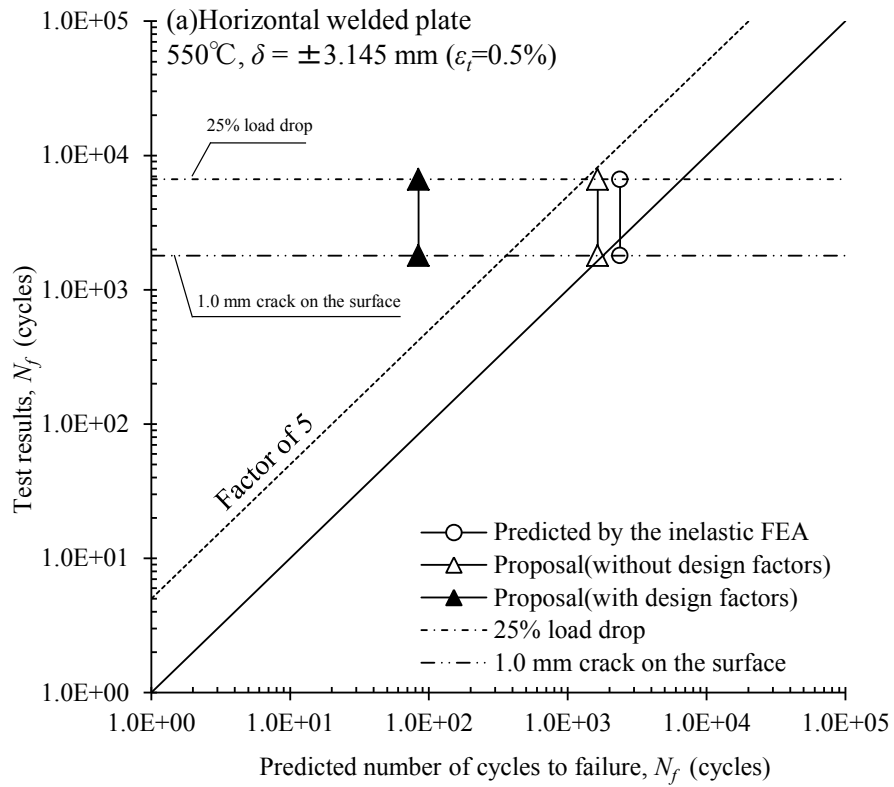




Fig.13

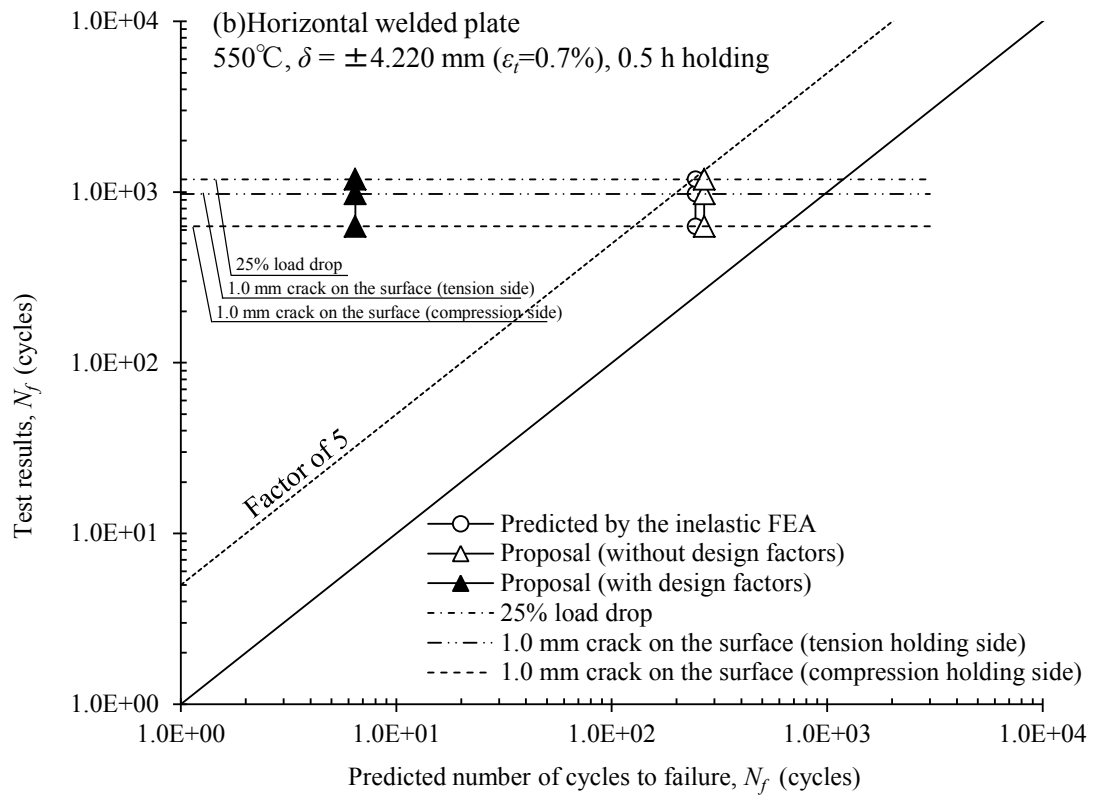
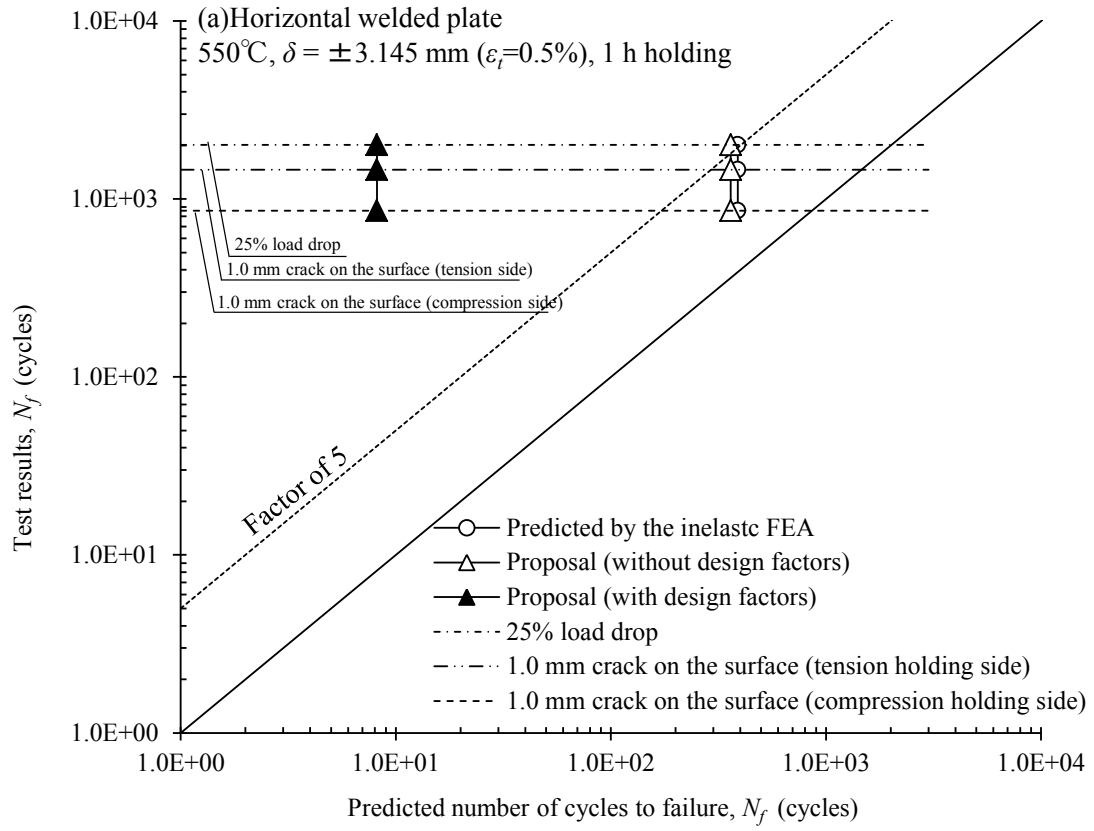


Fig.14

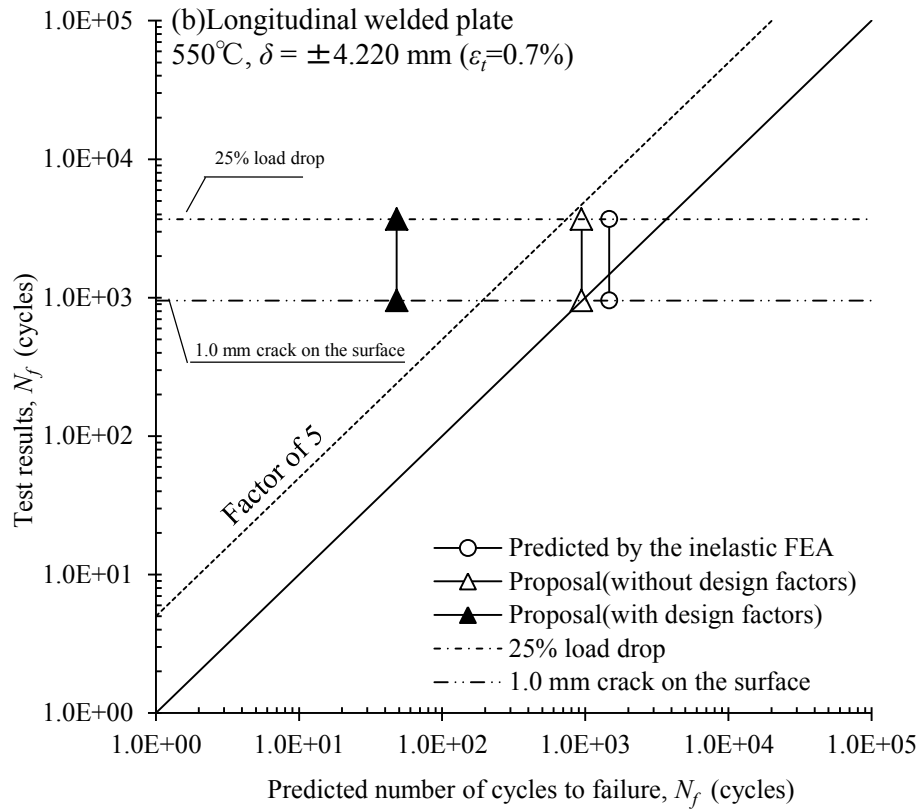
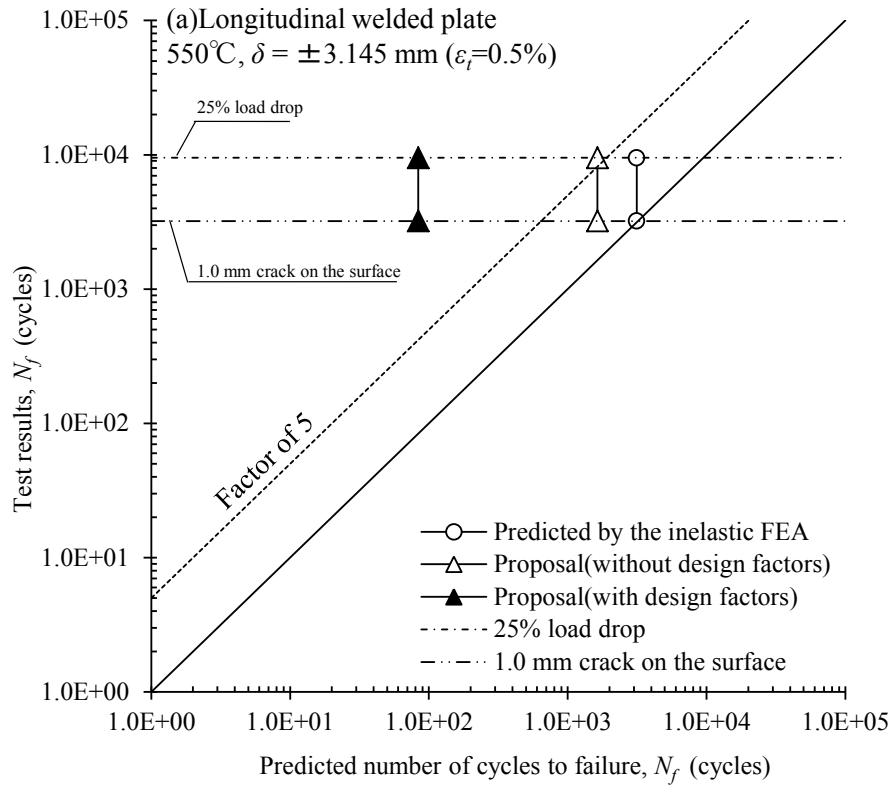
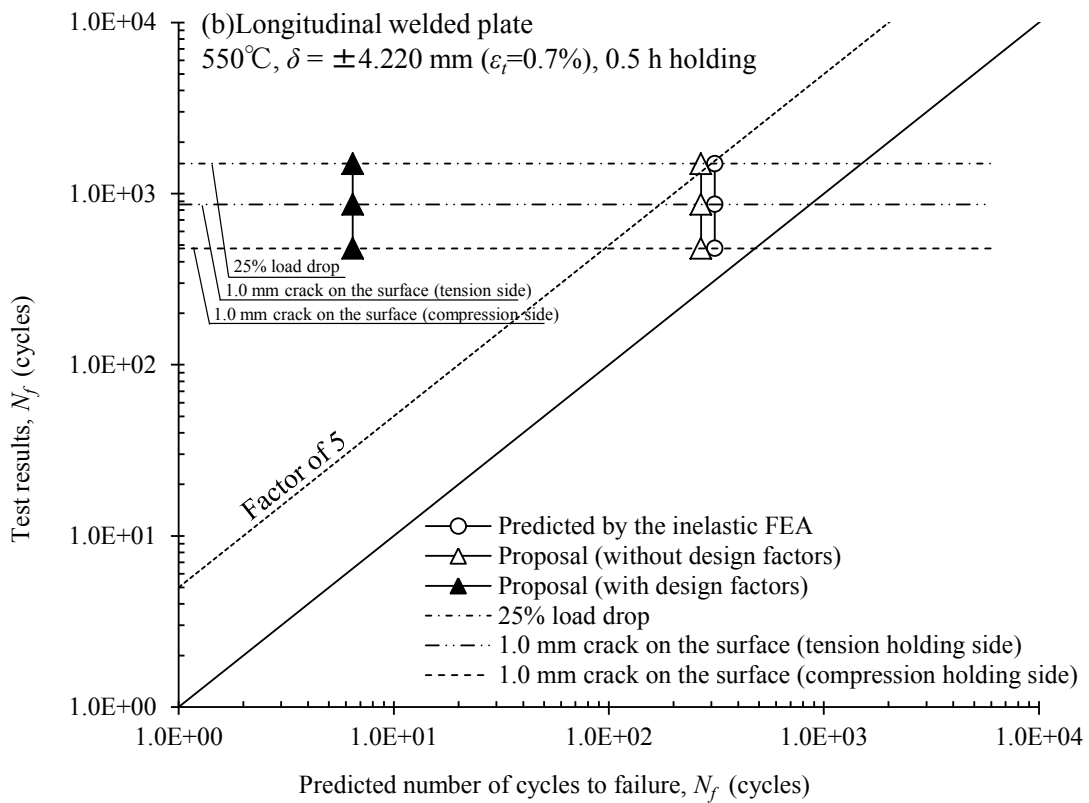
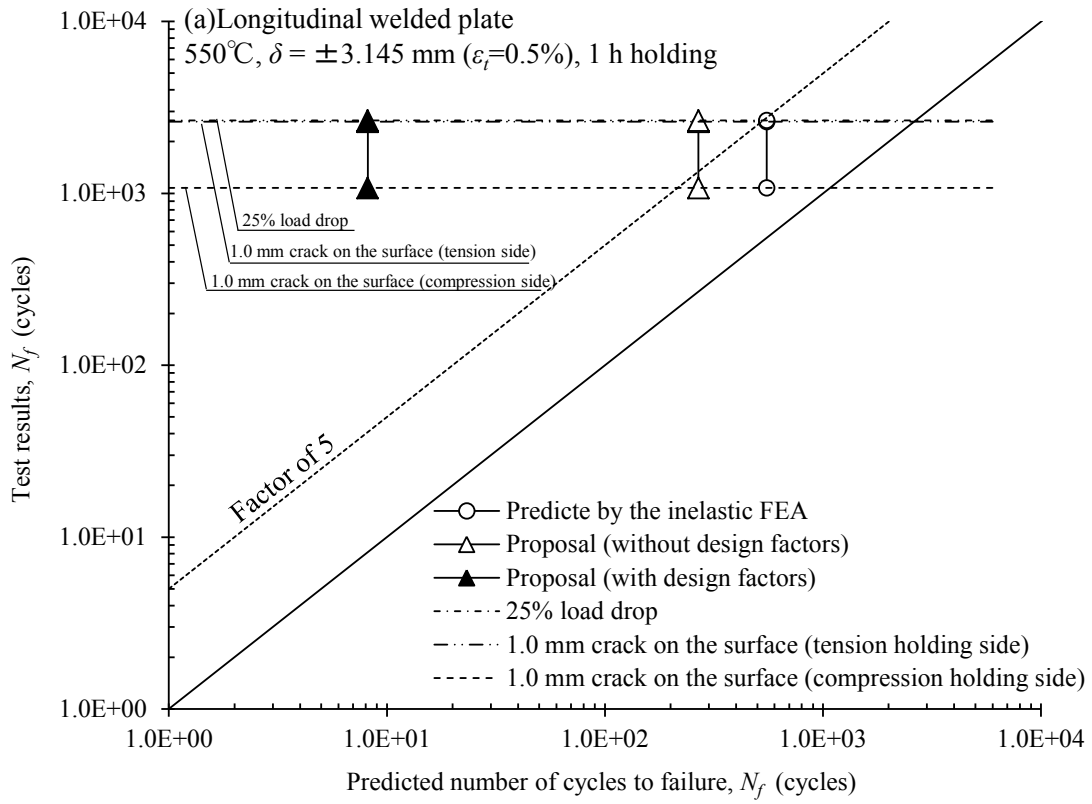


Fig.15



# Table list

Table 1 Chemical composition and heat treatment of the weld joint

Table 2 Results for the cyclic plate bending tests

Table 3 Results for the uniaxial creep-fatigue tests with surface observation

Table 4 Material properties assumed for the three materials modeled in the elemental inelastic FEA

Table 1

	C	Si	Mn	P	S	Ni	Cr	Mo	Nb	V	N	Cu
Base metal	0.10	0.35	0.43	0.012	0.001	0.05	8.53	0.98	0.08	0.20	0.048	-
Weld metal	0.08	0.16	0.99	0.008	0.007	0.70	8.94	0.89	0.04	0.17	-	0.12

Heat treatment for the BM: 1050 °C × 30 min + 780 °C × 30 min

Post welding heat treatment: 740 °C × 8.4 h

Table 2

Specimen	Temperature (°C)	Deformation amplitude (mm)	Holding time (hour)	Location	$N_{1.0\text{ mm}}$ ( <i>comp. side</i> ) (cycles)	$N_{1.0\text{ mm}}$ ( <i>tens. side</i> ) (cycles)	$N_{25\% \text{ drop}}$ (cycles)
Horizontal welded plate	550	3.145	0	BM/HAZ	Not observed	1800	6644
				WM		>6644	
		1.0	1.0	BM/HAZ	860	1460	2017
				WM	>2017	>2017	
		4.220	0	BM/HAZ	Not observed	498	1274
				WM		Not observed	
Longitudinal welded plate	550	3.145	0	BM/HAZ	Not observed	3210	9495
				WM		3700	
		1.0	1.0	BM/HAZ	1075	2610	2650
				WM	1165	1767	
		4.220	0	BM/HAZ	Not observed	Not observed	3687
				WM		954	
			0.5	BM/HAZ	478	864	1496
				WM	589	772	

Table 3

Temperature (°C)	Strain range (%)	Holding time (h)	Holding position	Observed location	$N_{l,0\text{ mm}}$ (cycles)	$N_f$ (cycles)
550	0.5	1.0	Compression	BM	1207	>1380
				WM	>1380	
			Tension	BM	1516(HAZ)	>1732
				WM	>1732	
	0.7	0.5	Compression	BM	561	>800
				WM	>800	
			Tension	BM	914(HAZ)	>1000
				WM	>1000	

Table 4

Item	BM	HAZ	WM
Elastic modulus	JSME FRs code[2]	= BM	= BM
Poisson's rate	JSME FRs code [2]	= BM	= BM
1/2 cyclic stress-strain response	Support document for the JSME FRs code [3]	= BM	$1.1 \times$ offset yield strength of the BM
Fatigue life	JSME FRs code [2]	= BM	$1.1 \times$ strain range with fatigue curve for the BM
Creep life	JSME FRs code [2]	$1/10 \times$ creep rupture time of the BM	= BM
Creep strain rate	JSME FRs code [2]	$1/10 \times$ creep rupture time of the BM	= BM